N71-15866
NASA CR-111840

ACOUSTIC RADIATION EFFICIENCY OF TRUNCATED CONICAL SHELLS

By

FREDERICK H. ELLINGTON and FRANKLIN D. HART

CASE FILE
COPY

ACOUSTIC RADIATION EFFICIENCY OF TRUNCATED CONICAL SHELLS

By Frederick H. Ellington and Franklin D. Hart

Prepared under Grant No. NGR-34-002-035 By

North Carolina State University

Raleigh, N. C.

For

National Aeronautics and Space Administration

SUMMARY

A combined analytical and experimental study is made of the acoustic radiation efficiency of a truncated conical shell. Previous work in the acoustic radiation efficiency of cylindrical shells is utilized in order to develop an approximating technique. The conical shell is then approximated by a series of cylindrical segments and the acoustic radiation efficiency of each segment is calculated. This method yields an upper bound solution for the acoustic radiation efficiency of truncated conical shells. The experimental program verifies the fact that the method yields an upper bound solution for the acoustic radiation efficiency.

TABLE OF CONTENTS

Page

LIST OF TABLES iv

LIST OF FIGURES v

INTRODUCTION 1

REVIEW OF LITERATURE 4

DEVELOPMENT OF MATHEMATICAL MODEL 6

General Comments on Acoustic Radiation 6
General Comments on Acoustic Radiation Resistance and Reactance 7

DYNAMICS OF SHELL STRUCTURES 13

Single Oscillator Response Analysis 13
General Shell Structural Vibration Patterns 17
Conical Shell Structure Vibration Patterns 18

METHOD OF CALCULATION OF ACOUSTIC RADIATION EFFICIENCY OF CYLINDERS 20

ACOUSTIC RADIATION EFFICIENCY OF TRUNCATED CONICAL SHELLS 29

Conical Shell Structure Represented by Equivalent Cylinders . . . 29
Computational Technique for Radiation Efficiency of Truncated Conical Shell 33

EXPERIMENTAL INVESTIGATION 50

Experimental Analysis of Parameters 50
Measurement of Radiation Resistance 53

Measurement of Acceleration Power Spectral Density 53
Measurement of Sound Pressure Power Spectral Density 54
Measurement of Reverberation Time of Acoustic Field 57
Measurement of Modal Density of Acoustic Field 57

Experimental Results 58

COMPARISON OF EXPERIMENTAL AND THEORETICAL RESULTS 59

SUMMARY AND CONCLUSIONS 60

LIST OF REFERENCES 62

APPENDIX. LIST OF SYMBOLS 63

LIST OF TABLES

Page

1. Structural and acoustical parameters for cylindrical shell 26

2. Structural and acoustical parameters for experimental conical shell 35

3. Cylindrical segment ring frequencies 36

4. Values of n_f and n_{tot} for cylindrical segments as a function of length 39

LIST OF FIGURES

Page

1. Hemispherical source in an infinite plane baffle 8
2. Radiation pattern for a piston at high ka 8
3. Radiation pattern for a piston when ka < 3.83 8
4. Flat piston with radiating elements 15
5. Frequency plot for a diffuse sound field 15
6. Frequency plot of diffuse sound field and an oscillator immersed in the field 15
7. Radiation efficiency calculation graph for cylinder 23
8. Geometry of truncated conical shell 31
9. Truncated conical shell with radius a and cylindrical segment which approximates the shell at frequency f_L 31
10. Truncated conical shell with intermediate radius a_i and corresponding approximating cylinder 31
11. Truncated conical shell immersed in a sound field with excitation frequency f_i 34
12. Experimental conical shell and approximating segments 34
13. Radiation efficiency calculation graph for a 6-inch cylindrical segment 38
14. Radiation efficiency calculation graph for a 12-inch cylindrical segment 40
15. Radiation efficiency calculation graph for an 18-inch cylindrical segment 41
16. Radiation efficiency calculation graph for a 24-inch cylindrical segment 42
17. Radiation efficiency calculation graph for a 30-inch cylindrical segment 43
18. Radiation efficiency calculation graph for a 36-inch cylindrical segment 44

LIST OF FIGURES (continued)

Page

19. Theoretical radiation efficiency for truncated conical shell divided into 6 segments 45

20. Theoretical radiation efficiency for truncated conical shell divided into 9 segments 47

21. Theoretical radiation efficiency for truncated conical shell divided into 12 segments 48

22. Theoretical and experimental radiation efficiency of truncated conical shell divided into 18 segments 49

23. Arbitrary structure receiving acoustic energy 52

24. Experimental apparatus to excite conical shell and record acceleration and sound pressure 55

25. Instrumentation and apparatus used in experimental program. . . 55

26. Reverberation time of test facility 56

INTRODUCTION

In this presentation, a twofold study is made of the vibrational and acoustical characteristics of truncated conical shells. Utilizing statistical energy concepts, an analytical-graphical technique is developed which determines the acoustical radiation efficiency of the truncated conical shell. An experimental study is also made to evaluate the accuracy of the analytical-graphical method.

The analytical-graphical method of evaluating the acoustical radiation efficiency of the truncated conical shell is developed by approximating the conical shell by a number of cylindrical segments varying in radii and lengths. The choice of cylindrical segment approximations depends upon the frequency range of interest. This method yields a set of values of acoustical radiation efficiency of the truncated conical shell which may be called upper bound values. The nature of the calculation is such that the determined valued of acoustic radiation efficiency are the maximum possible values at a given frequency.

The approximation technique involves choosing a cylindrical segment of the same thickness and material as the truncated conical shell and calculating its acoustic radiation efficiency. The method by which the cylindrical segment is chosen is of prime importance and will be described briefly here. The range of applicable frequencies is determined through a consideration of the frequency range lying between the lower ring frequency and the upper ring frequency of the conical shell. Then, for any frequency in this range, a cylindrical segment is chosen which has a ring frequency the same as the frequency in question. The

length of this cylindrical segment is chosen such that the defined cylinder length is equal to the length of the conical shell which has a radius greater than or equal to the radius of the cylinder mentioned previously. Thus, by choosing any frequency in the applicable range, the radius and length of the equivalent cylinder is specified.

Once the equivalent cylinder is defined, the acoustic radiation efficiency for that particular cylinder is calculated by the analytical-graphical technique. This value of radiation efficiency is the value assigned to the truncated conical shell at the frequency in question.

It is known that there is a peak in the acoustic radiation efficiency of a circular cylinder in the vicinity of the ring frequency so long as the ring frequency is less than the critical frequency. Because of this peak in radiation efficiency near the ring frequency, this solution technique yields an upper bound solution for the radiation efficiency.

The net result of the analytical-graphical determination is a graph of acoustic radiation efficiency versus frequency for a particular truncated conical shell.

The experimental investigation was carried out to determine the accuracy of the preceding operation and also to establish certain procedures governing the experimental technique. This experiment relied upon the determination of a group of parameters for the conical shell and using these quantities in an equation which determined the acoustic radiation efficiency.

The ability of being able to determine the acoustic radiation efficiency of a truncated conical shell is significant for a variety of

application purposes. In spacecraft, aircraft, landcraft, and undersea vehicles, conical shells are often used in the structural makeup. Because of the acoustical environment to which many of these structures are exposed, transmission and response phenomena are important. Structures thus mentioned can generate appreciable sound fields. They often receive appreciable energy from sound fields as well. Thus the coupling between a structure and a sound field is very significant. Knowledge of the acoustic radiation efficiency of these conical shell structures will provide much knowledge needed to predict the amount of acoustic energy that will accelerate a body and how much of that energy will be dissipated. This knowledge will also enable one to predict how much vibrational energy input to a structure will go to acoustic energy and how much will be dissipated.

The value of acoustic radiation efficiency is very significant in structural vibration work and it is felt that this presentation will be a valuable practical tool in determining acoustic radiation efficiency.

REVIEW OF LITERATURE

When a structure is immersed in a sound field, the vibrations of the structure and the sound field are coupled in a unique manner. A generalization of this phenomena has been discussed by Lyon and Maidanik (1962) through a consideration of the power flow between linearly coupled oscillators. In this study, the power flow between structural vibrational modes of an oscillator and a reverberant sound field was studied. Introducing the concept of equipartition of energy between the two classes of oscillators, they were able to quantify the parameter that couples the two vibrational fields and this parameter is referred to as the acoustic radiation resistance. They develop several theoretical expressions for the acoustic radiation efficiency of structures and another equation that is used widely in experimental determination of acoustic radiation efficiency.

Maidanik (1962) extended the analysis of structural vibrations to the behavior of flat panels in reverberant acoustic fields. He found that a statistical method for predicting the response of panels in reverberant acoustic fields could be utilized giving good practical results. He showed that the acceleration spectrum of the vibrating panel was related to the pressure spectrum of the reverberant field by a coupling factor which is a simple function of radiation and mechanical resistance of the structure. The overall aim of this work was to estimate the response of the structure when it was immersed in a reverberant acoustical field, knowing the gross structural parameters. This analysis considered the power radiated from a vibrating panel and

related it to the acoustic radiation resistance. The modal behavior of plates is discussed and the work finishes with the development of an experimental equation whereby the radiation resistance of a panel can be determined from experimental data.

A later analysis was carried out by Manning and Maidanik (1964) in which a theoretical approach was developed similar to that done by Maidanik (1962) except it developed the radiation efficiency of cylindrical shells. A statistical-graphical technique was developed which yielded the acoustic radiation efficiency of a cylindrical shell. This statistical-graphical approach gave a theoretical solution which was verified by an experimental program similar to those previously done. The major consequence of this research was that it extended theory which had previously been restricted for use on flat panels to three-dimensional structures, that is cylindrical shells.

DEVELOPMENT OF MATHEMATICAL MODEL

General Comments on Acoustic Radiation

The simplest type of acoustic radiation normally encountered is that from a pulsating sphere in a non-reflecting environment. This is a sphere whose radius varies in length sinusoidally with time. Many acoustic radiators behave similar to pulsating spheres if their significant dimensions are small compared to the acoustic wavelength of the radiated sound. Quantities such as the acoustic pressure generated, particle velocity, source strength, acoustic wave intensity, power radiated, and other significant parameters can readily be computed for the pulsating sphere (Kinsler and Frey, 1962).

Slightly more complex than the simple spherical source is the simple source in an infinite baffle in an environment with non-reflecting boundaries. Here, acoustic radiation is confined to one side of the plane. One model of this would be the hemispherical source if it were in an infinite plane baffle as shown in Figure 1.

Many of the equations governing the acoustic parameters of the simple pulsating sphere can be modified to yield equations for the hemisphere in the infinite baffle. It can be easily verified (Kinsler and Frey, 1962) that the pressure produced by hemispherical source in an infinite baffle is twice as great as that produced by a spherical source of the same strength. Kinsler and Frey (1962) also derive the expressions for acoustic power and intensity for the hemisphere in an infinite baffle.

Acoustic radiation from an extended surface does not have the symmetric radiation patterns as does the simple source. Such is the

case concerning acoustic radiation from a vibrating piston. The pressure produced at any point in an acoustic medium by such a surface is determined by summing the discrete pressures which would be produced by an equivalent array of simple sources. Theoretically, one could determine the pressure produced by such a vibrating body by formulating a differential pressure and integrating it over the surface of the body. The mathematical difficulties encountered in this method are, however, very great except in the more simple cases.

The nature of the kinds of approximations that can be made concerning acoustic radiation, while maintaining adequate numerical description, can be illustrated through a discussion of the piston problem. When the piston radius is large compared to acoustic wavelength, that is when $ka \gg 1$, where k is the wave number and a is the radius of the piston, the radiation pattern of the piston is shown by Kinsler and Frey (1962) to be like that in Figure 2. Obviously, when ka is small, the directivity factor approaches unity for all angles, and the pressure amplitudes approach those of a hemispherically radiating source of the same strength. This fact can be ascertained from Figure 3 and Kinsler and Frey (1962). Thus for small ka, the flat piston acts essentially like a simple source.

General Comments on Acoustic Radiation Resistance and Reactance

In the preceding developments the main concern was the development of pressures and intensities of acoustic waves set up in a medium surrounding a vibrating source. The main parameters needed were assumed to be known. These parameters were the amplitude and the frequency of

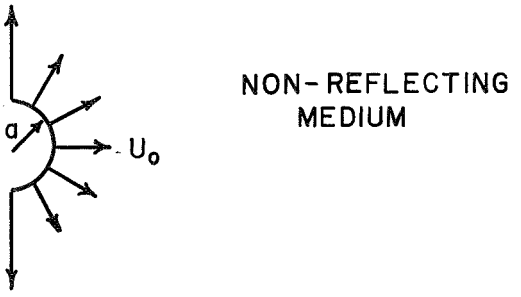

FIGURE 1. HEMISPHERICAL SOURCE IN AN INFINITE PLANE BAFFLE

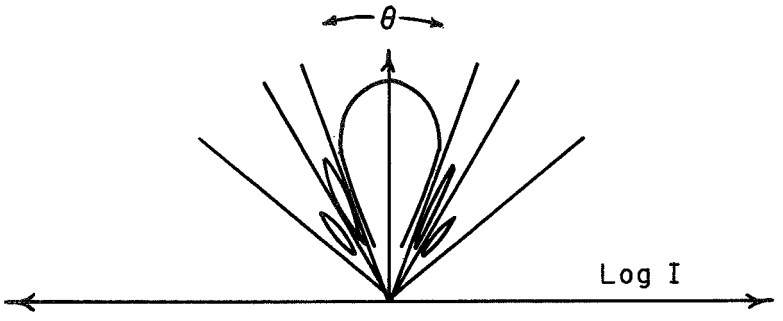

FIGURE 2. RADIATION PATTERN FOR A PISTON AT HIGH ka

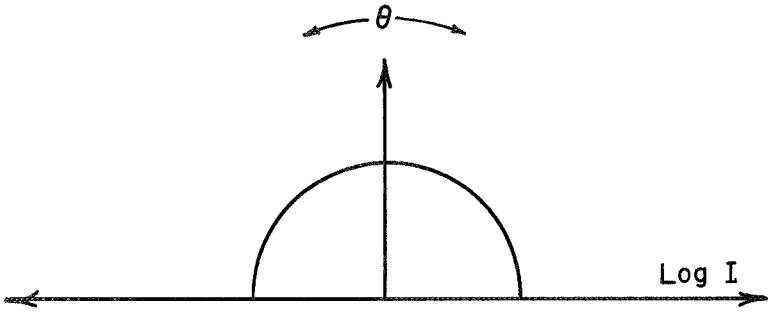

FIGURE 3. RADIATION FOR A PISTON WHEN $ka < 3.83$

vibration of the surface. In practical problems, often neither of these two parameters are shown, but, many times what is known is the driving force or the driving power. Under such circumstances, the amplitude of vibration is a function of frequency. Consequently, the dynamic constants of the driver are needed as expected, but, in addition, the reaction force with which the medium acts on the surface of the body are needed. To illustrate this concept of reaction force and to give an intuitive feel for the interaction of the fluid medium on the surface, the piston is used as a model.

Consider two elements of area dS and dS', on a piston. Let dp be the pressure increment that dS produces in the medium at a point in the medium at a point adjacent to dS'. To find the acoustic pressure in the medium adjacent to dS', Kinsler and Frey (1962) integrate over the piston to get:

$$\bar{p} = \iint \frac{j\rho_o ckU_o}{2\pi r} e^{j(\omega t - kr)} \, dS \tag{1}$$

where r is the distance between dS and dS'. This piston is shown in Figure 4. The total reaction force acting on a piston is,

$$\bar{f}_r = -\iint \bar{p} dS' \, . \tag{2}$$

Substituting the value of p from equation (1) into equation (2) yields:

$$\bar{f}_r = -\frac{j\rho_o ckU_o e^{j\omega t}}{2\pi} \iint dS' \iint \frac{e^{-jkr}}{r} \, dS \, . \tag{3}$$

Kinsler and Frey (1962) integrate the preceding equation to get:

$$\bar{f}_r = -\rho_o c\pi a^2 U_o e^{j\omega t}(R_1(2ka) + jX_1(2ka)) \tag{4}$$

and also define $R_1(x)$ and $X_1(x)$ to be:

$$R_1(x) = \frac{x^2}{2\cdot 4} - \frac{x^4}{2\cdot 4^2\cdot 6} + \frac{x^6}{2\cdot 4^2\cdot 6^2\cdot 8} - \cdots , \tag{5}$$

$$X_1(x) = \frac{4}{\pi}\left(\frac{x}{3} - \frac{x^3}{3^2\cdot 5} + \frac{x^5}{3^2\cdot 5^2\cdot 7} - \cdots\right) . \tag{6}$$

$R_1(x)$ is called the piston radiation resistance function and $X_1(x)$ is called the piston radiation reactance function. To determine the acoustic radiation efficiency of this piston, a function of equation (5) must be divided by the radiation resistance of a flat plate with high ka. The divisor is $\rho_o c_o A$, where ρ_o is the ambient density of the sound field, c_o is the speed of sound in the surrounding medium and A is the area of the piston.

Assuming small ka for the piston as discussed previously, $R_1(x)$ and $X_1(x)$ are approximated by the first term in equation (5) and equation (6). Thus

$$R_1(x) \approx \frac{x^2}{8} , \tag{7}$$

$$X_1(x) \approx \frac{4x}{3\pi} . \tag{8}$$

When x or ka is large, it can be shown (Kinsler and Frey, 1962) that equation (5) and equation (6) reduce to

$$R_1(x) \approx 1 \tag{9}$$

and

$$X_1(x) \approx \frac{4}{\pi} x . \tag{10}$$

Tables are often used for determining the acoustic radiation resistance function and the acoustic radiation reactance function for pistons. It is clear that knowing the radiation resistance of a piston or any other object, its radiation efficiency can be determined.

Another important parameter is acoustic radiation impedance, Z_r. This is the ratio of the force exerted by a surface on its surrounding acoustic medium to the velocity of that surface. For the piston, the force has been defined in equation (4). Since the velocity of the piston is

$$u = U_o e^{j\omega t} \tag{11}$$

then the radiation impedance is

$$Z_r = \frac{-\bar{f}_r}{U_o e^{j\omega t}} = \rho_o c \pi a^2 \left[R_1(2ka) + jX_1(2ka)\right] . \tag{12}$$

The real part of Z_r is the radiation resistance and the imaginary part is the radiation reactance. As mentioned previously, the radiation efficiency of the piston is the ratio obtained by dividing the real part of equation (12) by $\rho_o c_o A$. If radiation efficiency is denoted by σ, then, for a piston,

$$\sigma = \pi a(R_1(2ka)) . \tag{13}$$

The radiation impedance is useful in determining the reaction force on the piston. This force is,

$$\bar{f}_r = -Z_r U_o e^{j\omega t} . \tag{14}$$

The acoustic power radiated from a body such as a piston is equal to the rate of doing work against the radiation resistance R_{rad}. The average power generated is

$$W = \tfrac{1}{2}R_{rad}U_o^2 \quad , \tag{15}$$

or

$$W = (\tfrac{1}{2})\rho_o c\pi a^2 U_o R_1(2ka) \quad . \tag{16}$$

Obviously, the preceding equations apply only to pistons and to structures which may be approximated by pistons, but they serve as a basis for further discussion of the concept of acoustic radiation.

DYNAMICS OF SHELL STRUCTURES

Single Oscillator Response Analysis

An explanation of how a simple oscillator radiates sound into a surrounding acoustic medium has been described in the preceding section. This simple source can be visualized as an analog to more complicated systems. Another analog can be used to represent acoustical systems. This analog is the linearly coupled oscillator. This analog is applicable both to simple and complex systems. It has merit because it utilizes the energy flow between the oscillator and its surrounding medium.

A reverberant acoustical field is one in which the sound is diffuse regardless of location in the field. The study of acoustical systems interacting with reverberant acoustic fields has been analyzed by Lyon and Maidanik (1962). The oscillators spoken of here are in reality the structure and the sound field. Thus there is a power flow between the structure and the acoustic field. Lyon and Maidanik (1962) use another analogy to find the power flow between the structure and the sound field. This second analogy is the thermal bath. The structure is considered to be a source of heat and it is immersed in a fluid which represents the acoustic medium. A net heat flow results between the heat source and the fluid and it is shown to be representative of the power flow between a sound source and its acoustic field. Power flows between the vibrating modes of the structure and the modes of the reberberant field

To illustrate the concept of the power flow between the oscillators, consider an oscillator in a diffuse sound field as shown in

Figure 5. Suppose the oscillator which is immersed in this field resonates at a frequency ω_1 as shown in Figure 6. At frequency ω_1, the spectral density of the mean square pressure is given by Lyon and Maidanik (1962) to be

$$S_p(\omega_1) = < p^2 > / \Delta\omega \quad . \tag{17}$$

The frequency ω_1 is the only frequency which the oscillator senses. With respect to the thermal analogy, the sound field in this interval has a temperature related to the spectral density and the systems will reach steady-state vibrations only at that temperature corresponding to ω_1.

Lyon and Maikanik (1962) also state that in a reverberant room of volume V the acoustic energy is

$$E_r = < p^2 > V \; / \; \rho_o c^2 \; . \tag{18}$$

This acoustic energy is divided into $n_r(\omega)\Delta\omega$ modes of the room. Here, $n_r(\omega)$ is the modal density of the room. Thus the average energy per mode is

$$\frac{E_r}{n_r(\omega)\Delta\omega} = \frac{< p^2 > V}{\rho_o c^2 n_r(\omega)\Delta\omega} = \frac{S_p(\omega) V}{\rho_o c^2 n_r(\omega)} \quad . \tag{19}$$

An expression for the modal density of a room is (Morse and Bolt, 1944)

$$n_r(\omega) = \frac{\omega^2 V}{2\pi^2 c^3} \quad . \tag{20}$$

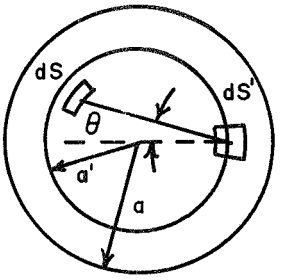

FIGURE 4. FLAT PISTON WITH RADIATING ELEMENTS

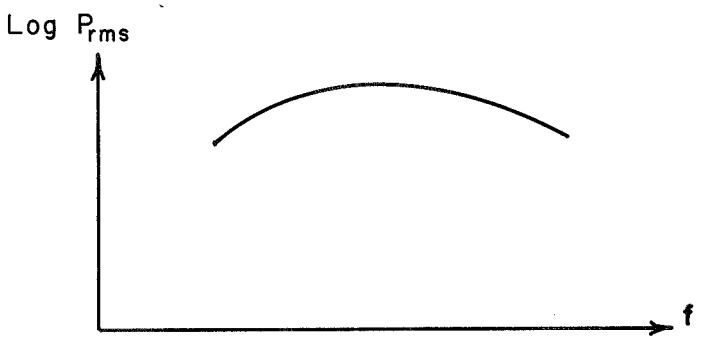

FIGURE 5. FREQUENCY PLOT FOR A DIFFUSE SOUND FIELD

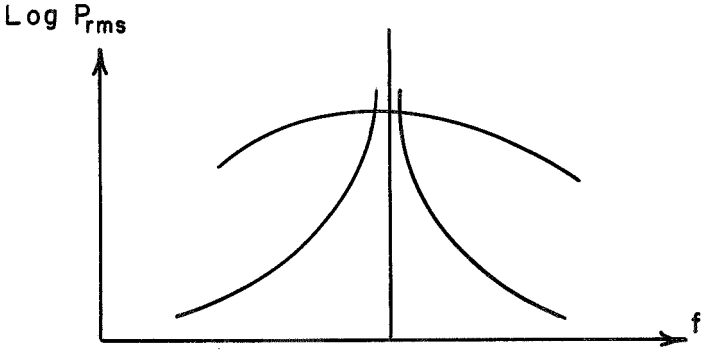

FIGURE 6. FREQUENCY PLOT OF DIFFUSE SOUND FIELD AND AN OSCILLATOR IMMERSED IN THE FIELD

Therefore the average energy per mode can be expressed as

$$\theta^R(\omega) = \frac{S_p(\omega)\, 2\pi^2 c}{\rho\omega^2} \quad .$$

In order to illustrate the heat analogy, let $\theta_r = KT$ where K is Boltzmann's constant and T is the temperature. Thus, in the thermal analogy, the oscillators have a given temperature which is a function of their frequency and amplitude.

If a mechanical oscillator is placed in a sound field it will interact with oscillators which represent this field and a net power flow will result between the two. The interaction between the mechanical oscillator and the field oscillators is confined mainly to the oscillators of the field which oscillate in a frequency band centered around the natural frequency of the oscillator. If a number of mechanical oscillators are placed in a field, the same type of interaction will result. Each of the mechanical oscillators will oscillate around its resonant frequency.

A structure consisting of many modes may be thought of as being a number of oscillators. For such a structure Lyon and Maidanik (1962) give its average energy per mode as:

$$\theta^s(\omega) = S_a(\omega) \;/\; (\omega n_s(\omega)) \tag{22}$$

where $n_s(\omega)$ is the structure modal density. Further, Lyon and Maidanik (1962) show that when a structure alone generates a reverberant sound field, the radiation resistance can be given by

$$R_{rad} = \{S_p(\omega) \;/\; S_a(\omega)\} \frac{c}{\rho} \beta_R \; (2\pi^2 n_R(\omega)) \tag{23}$$

and the radiation efficiency of the structure in this case is

$$\sigma = \{S_p(\omega) \ / \ S_a(\omega)\} \frac{1}{\rho^2 a} \beta_R \ (2\pi^2 n_R(\omega)) \ . \tag{24}$$

Thus the steady state relations for the flow into and from a structure in an acoustic environment may be predicted by use of equations (23) and (24).

General Shell Structural Vibration Patterns

When considering acoustic radiation from shells, the characteristics of the shell vibration patterns are important. The amount and characteristics of the acoustic radiation from shells is directly affected by the vibration patterns which produces the radiation. A strip mode in a shell is a mode of vibration which looks like a strip on the shell surface. Acoustic energy is radiated from such a vibrating strip. A piston mode on a shell is a mode of vibration of the shell which radiates acoustic energy from that portion of the shell similar to the way a vibrating piston would if it were in the same position as the piston mode. A circumferential strip mode on a shell would be the strip which would go around the shell at any circumference. This circumferential strip mode would produce acoustic radiation similar to a vibrating ring segment around the shell's circumference. Circumferential strip modes are often found in cylinders. Axial-strip modes are modes which may be visualized as strips on the surface of a shell oriented in a direction parallel to the axis of the shell.

The need for the classification of vibrational modes in shells is obvious. When these modes are separated from each other and classified,

they may be analyzed more efficiently. That is, if all the strip modes in a vibrating shell could be distinguished, they could be analyzed simply as radiating strips. If all the piston modes in a shell could be isolated and characterized, they could be treated as an array of piston radiators. The ability of being able to categorize the types of modes becomes obvious when the different types of radiation from each of these modes is analyzed. That is, the radiation from piston modes has typical characteristics which may be analyzed. The radiation from strips has characteristics which differ with that from pistons and this strip radiation may also be analyzed by treating it separately.

Thus, once the radiation from a shell may be categorized by the radiators which produce it, the modal radiation analyses may be extended further. This fact will become evident in a following section which makes use of the categorization of radiating modes into circumferential-strip modes, axial strip modes and piston modes.

Conical Shell Structure Vibration Patterns

The acoustic radiation which a conical shell produces is dependent upon the vibration patterns producing the radiation. Around the circumference of the conical shell there exist modes which are circumferential-strip radiators. Down the axis of the conical shell there exist modes which are axial-strip radiators. At the edges of the shell are coner modes which are corner radiators. At high frequencies, where many modes are uncoupled, there exist piston modes which radiate like piston radiators.

The radiating modes of a conical shell are strongly affected by structural characteristics of the shell. Curvature along the circumference of the conical shell affects the behavior of the circumferential-strip modes. Curvature effects make some circumferential-strip modes increase in their flexural-wave speed. End discontinuities affect axial-strip modes and sometime cause them to behave like piston modes in the region of the discontinuity. Once the different modes which exist in a conical shell may be separated from each other, an examination of the radiation they produce may be made. Thus it is of prime importance to be able to distinguish the different vibration modes which occur in a vibrating piston.

METHOD OF CALCULATION OF ACOUSTIC RADIATION EFFICIENCY OF CYLINDERS

Manning and Maidanik (1964) develop an analytic method by which the radiation efficiency of cylinders can be calculated. The author has analyzed this method and has extended the technique to broader cylinder radiation analyses. In the presentation by Manning and Maidanik (1964) an example of the determination of the radiation efficiency by theoretical means is presented. That particular analysis will be presented here in much greater detail in order to clarify the theoretical method of determining acoustic radiation efficiency of cylinders. This example of calculation of acoustic radiation efficiency should help clarify the techniques of analysis of acoustic radiation efficiency of truncated conical shells.

A technique of computing the radiative properties of flat panels developed by Maidanik (1962) showed that the use of typical modal vibration patterns could yield good values of acoustic radiation efficiency. In order to perform this analysis the vibrational modes of the structure had to be classified. The classifications were (1) acoustically fast modes, where $c_b \geq c_o$ for which $\sigma_f \approx 1$, and (2) acoustically slow modes where $c_b < c_o$. Strip modes and piston modes make up the acoustically slow modes. Strip modes are modes whose vibrational characteristics can be represented by a vibrating strip and piston modes are modes whose vibrational characteristics can be represented by a vibrating piston. The acoustically fast and acoustically slow modes were determined by an investigation of the frequency equation of the structure.

The work done by Maidanik (1962) was inadequate for the analysis of cylindrical shells. The reason for this inadequacy was the fact that the analysis did not consider the effects of curvature on acoustically fast and acoustically slow modes. With certain modifications for curvature, the technique can be used for analysis of acoustic radiation from cylinders.

To investigate the effect of curvature upon the modal radiation of a cylinder, consider the frequency equation of a cylinder developed by Heckl (1962),

$$\nu^2 = \frac{h^2 a^2}{12} (K_x^2 + K_y^2)^2 + (1-\mu^2) \left(\frac{K_y^4}{(K_x^2 + K_y^2)^2}\right) . \tag{25}$$

In this equation the circumferential wave number is given by K_x where,

$$K_x = \frac{2\pi}{\lambda_x} , \tag{26}$$

$$\lambda_x = \frac{2\pi a}{n} , \tag{27}$$

$$cir = 2\pi a , \tag{28}$$

so that

$$K_x = n/a . \tag{29}$$

Also, the axial wave number k_y is given by

$$K_y = \frac{2\pi}{\lambda_y} \tag{30}$$

where

$$\lambda_y = \frac{L}{m/2} \tag{31}$$

so that

$$K_y = \frac{m\pi}{L} \quad . \tag{32}$$

Substituting equations (29) and (32) into equation (25) yields,

$$\nu^2 = \frac{h^2 a^2}{12} \left\{ \left(\frac{n}{a}\right)^2 + \left(\frac{m\pi}{L}\right)^2 \right\} + (1-\mu^2) \left\{ \frac{\left(\frac{m\pi}{L}\right)^4}{\left[\left(\frac{n}{a}\right)^2 + \left(\frac{m\pi}{L}\right)^2\right]^2} \right\} . \tag{33}$$

Equation (33) is the frequency equation for a cylinder in terms of the mode numbers m and n. Equation (33) is shown plotted in Figure 7 for a particular cylinder.

Continuing with the cylinder's modal modification, Manning and Maidanik (1964) explain that if the cylinder is represented by an equivalent plate, the only vibrational modes which radiate in the equivalent-plate formalism are the circumferential-strip modes. These circumferential-strip modes satisfy the relation,

$$aK_x = \frac{C_L}{c_o} \nu \tag{34}$$

Equation (34) is also plotted on Figure 7 and is designated by a dashed line. Manning and Maidanik (1964) describe that the modes which lie to the right of this line are the only ones which radiate if the cylinder is considered to be an equivalent plate.

To establish the region in which the circumferential-strip modes exist, a parameter which is called the critical frequency must be defined. This is the frequency at which the flexural-wave speed in a flat panel of thickness equal to that of the structure in question is equal to the speed of sound in the surrounding acoustic medium. The

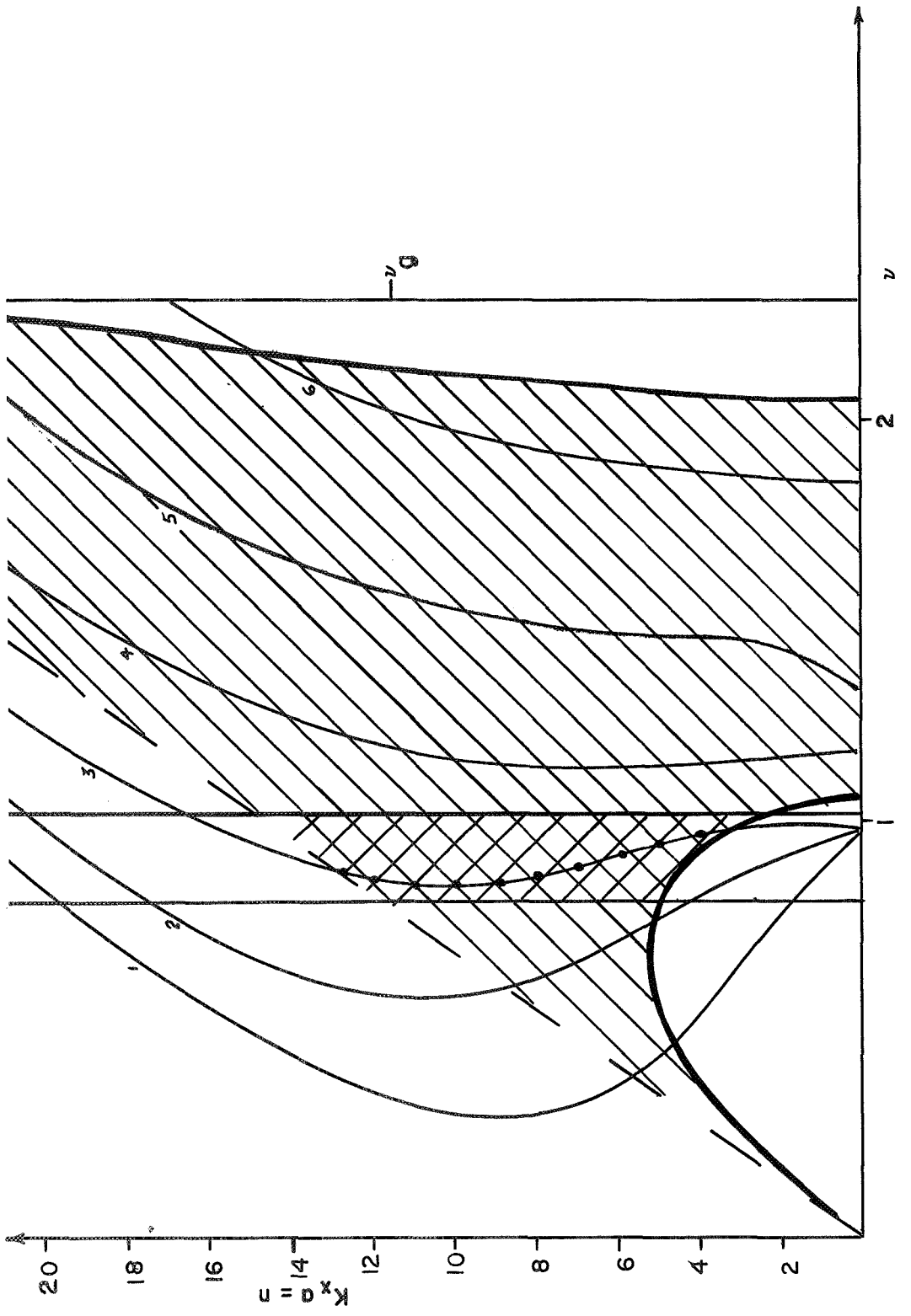

FIGURE 7. RADIATION EFFICIENCY CALCULATION GRAPH FOR CYLINDER

critical frequency is given by

$$\nu_g = \frac{c_o^2}{1.8hc_L f_r} \tag{35}$$

where f_r is the ring frequency of the cylindrical segment and f_r is the frequency at which the longitudinal wavelength in the cylinder material is equal to its circumference. Equation (35) is shown plotted in Figure 7 and is the vertical line labeled ν_g. Thus, according to Manning and Maidanik (1964) all modes lying on Figure 7 to the left of the line labeled ν_g and to the right of the curve of equation (34) are circumferential-strip modes in the equivalent-plate formalism.

As mentioned previously, the equivalent-plate formalism is inadequate for cylinders because it lacks curvature modifications. Some modification of Figure 7 must be made to account for curvature. Manning and Maidanik (1964) determine the modification for curvature. They say that some of the circumferential-strip modes are altered by curvature effects to the extent that they become acoustically fast modes. They say that modes satisfying the relation,

$$ak_x \geq \frac{c_L}{c_o} \nu \text{ Re } [\{(1-\mu^2)^{\frac{1}{2}} - \nu [1 - (\frac{\nu}{\nu_g})^2]^{\frac{1}{2}}\}^{\frac{1}{2}}] \tag{36}$$

as well as satisfying the previously stated requirements for circumferential-strip modes, are acoustically fast modes. The radiation efficiencies for the acoustically fast modes is approximately unity. Equation (36) then constitutes the modification for curvature. The plot of equation (36) is shown in Figure 7 by the heavy dark line. The region to the right of the curve of equation (34), above the curve

of equation (36), and to the left of the line ν_g contains only acoustically fast modes with radiation efficiency approaching unity.

As previously stated, the radiation efficiency of acoustically fast modes is much greater than that of circumferential-strip modes. Thus, in the range of frequencies where acoustically fast modes exist, the radiation efficiency of the structure is controlled mainly by those acoustically fast modes. It is for this reason that Manning and Maidanik (1964) say that in this region

$$\sigma \approx \frac{n_f}{n_{tot}} \tag{37}$$

where n_f is the total number of acoustically fast modes lying in that frequency band and n_{tot} is the total number of modes in that same band.

Using the equations (33), (34), (35) and (36), a graph like the one shown in Figure 7 can be constructed for a particular cylinder. The acoustic radiation efficiency can then be calculated from this graph alone. The calculation procedure is to select a band of frequencies of interest and outline it on the graph. In that band, count n_f and n_{tot} and then use these values in equation (37).

Manning and Maidanik (1964) present an example determination of the acoustic radiation efficiency of a cylinder. That calculation is repeated here in greater detail for illustrative purposes. The radiation efficiency of the same cylinder will be determined near its ring frequency. The structural parameters of this cylinder are shown in Table 1.

Table 1. Structural and acoustical parameters for cylindrical shell

Shape	cylindrical shell
Material	steel
Length (L)	24 inches
Radius (a)	18 inches
Thickness (h)	0.125 inch
Young's Modulus (E)	27.6×10^6 lb_f/in^2
Density (ρ)	0.28 lbm/in^3
Ring Frequency	1,726 Hz
Critical Frequency	3,986 Hz
Velocity of Wave Propagation (C_L)	1.952×10^5 in/sec
Poisson's Ratio (μ)	0.3
Dimensionless Critical Frequency $\nu_g = f_g/f_r$	2.31
Medium	Air
Air Density (ρ_o)	0.077 lbm/ft^3
Local Speed of Sound (c_o)	13,550 in/sec

The frequency band in which the acoustic radiation efficiency will be calculated is the 1/3 octave band which encloses the ring frequency of 1726 Hz. This band covers the frequency range of from 1416 Hz to 1784 Hz or from $\nu = 0.82$ to $\nu = 1.03$ as seen on Figure 7. Using the cylinder's structural parameters, equations (33), (34), (35) and (36) are plotted on Figure 7.

On Figure 7 the region which contains the acoustically fast modes is cross hatched. The region from $\nu = 0.82$ to $\nu = 1.03$ which contains the acoustically fast modes is double cross hatched. This double cross-hatched region is the area from which n_f will come. The points in this area where the frequency equation curves (labeled m = 1,2,...) intersect with the integral values of circumferential mode numbers will be designated with dark dots. The total number of these dots determines n_f. Counting these dots indicates that $n_f = 10$. Outside the double cross-hatched area, but between $\nu = 0.82$ and $\nu = 1.03$, the other points where the frequency equation curves intersect the integral values of circumferential mode number are counted. These number of intersections are added to get n_{tot}. Since there are 16 of these other intersections,

$$n_{tot} = n_f + 16 \tag{38}$$

so

$$n_{tot} = 10 + 16 = 26 \ . \tag{39}$$

Thus utilizing equation (37),

$$\sigma = \frac{10}{26} = 0.39 \ . \tag{40}$$

One customary way to express radiation efficiency is on a logarithmic scale. The value in this case is

$$10 \log_{10} \sigma = -4 \ . \tag{41}$$

Thus equations (40) and (41) express the acoustic radiation efficiency of the cylindrical shell in the one-third octave band centered at 1600 Hz. These results are the same as those found by Manning and Maidanik (1964).

The purpose of the preceding example has been to clarify the work done by Manning and Maidanik (1964) and to serve as a basis for the determination of the radiation efficiency of the truncated conical shell.

ACOUSTIC RADIATION EFFICIENCY OF TRUNCATED CONICAL SHELLS

Conical Shell Structure Represented by Equivalent Cylinders

When a truncated conical shell is immersed in a diffuse sound field, it will vibrate with that field around certain frequencies. This range of frequencies is of concern with respect to the determination of acoustic radiation efficiency. The geometry of a typical truncated conical shell is shown in Figure 8. This conical shell possesses an upper and a lower ring frequency. A ring frequency is a frequency of vibration of the conical shell at which the longitudinal wavelength of the wave in the conical shell material is equal to a given circumference. Obviously, since the radius, and hence the circumference, of the conical shell, vary infinitely between the smaller and larger radii, there exist an infinite number of different ring frequencies in a conical shell. The two ring frequencies corresponding to the smallest and largest diameter are the upper and lower ring frequencies, respectively. It is in the range of frequencies between the upper and lower ring frequencies that the investigation of acoustic radiation efficiency will be conducted.

The approximation of the truncated conical shell will be made by starting at f_L, the lower ring frequency and approximating the conical shell by a cylindrical segment with the same thickness and made of the same material as the conical shell. The length of this segment will be chosen to give a reasonable approximation. The radius of this segment is defined as the radius of the conical shell corresponding to f_L. The radiation efficiency of the conical shell seen in Figure 9a at the

frequency f_L is approximated by the radiation efficiency of the cylindrical segment shown in Figure 9b.

For a frequency f_i between f_L and f_u, the following holds as the approximation procedure:

(1) Determine the frequency f_i needed.

(2) Find the radius of a cylinder of the same material and thickness as the conical shell with ring frequency f_i.

(3) Signify this radius a_i (see Figure 10b).

(4) Find the length of the cylindrical segment, L_i, governed by a_i (see Figure 10b).

(5) The radiation efficiency of the truncated conical shell at frequency f_i will be approximated by the radiation efficiency of the cylinder (see Figure 10b).

The maximum frequency for which a value of radiation efficiency can be calculated by this method is f_u, the upper ring frequency. Above f_u it is deduced that the radiation efficiency of the truncated conical should approach unity since Miller (1969) says that above the upper ring frequency the modal behavior of the truncated conical shell is the same as that of a flat plate. The aim of the preceding procedure is to determine a set of upper bound values for the acoustic radiation efficiency of the truncated conical shell. It has been shown[1] that a truncated conical shell may be approximated by a series

---

[1]K. L. Chandiramani, Bolt Beranek and Newman, Inc. (Cambridge, Massachusetts). 1967. Response of a conical shell to a turbulent boundary layer pressure field. Paper presented at the 74th meeting of the Acoustical Society of America in Miami Beach, Florida.

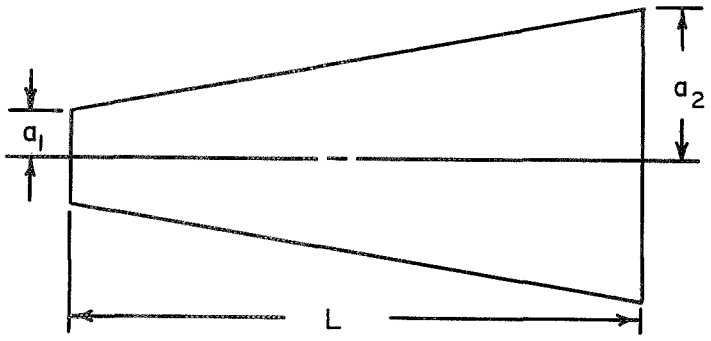

FIGURE 8. GEOMETRY OF TRUNCATED CONICAL SHELL

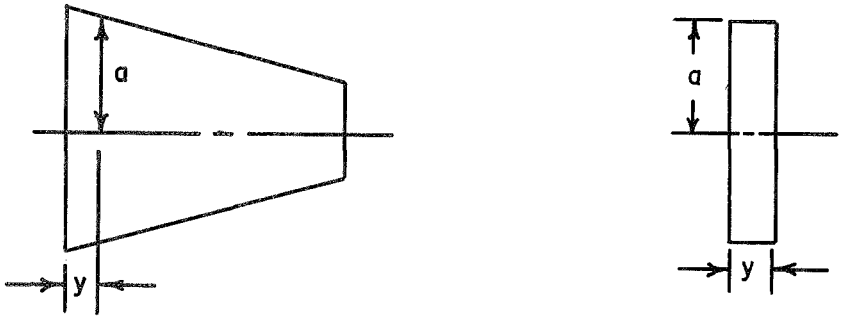

FIGURE 9. TRUNCATED CONICAL SHELL WITH RADIUS a AND CYLINDRICAL SEGMENT WHICH APPROXIMATES THE SHELL AT FREQUENCY f_L

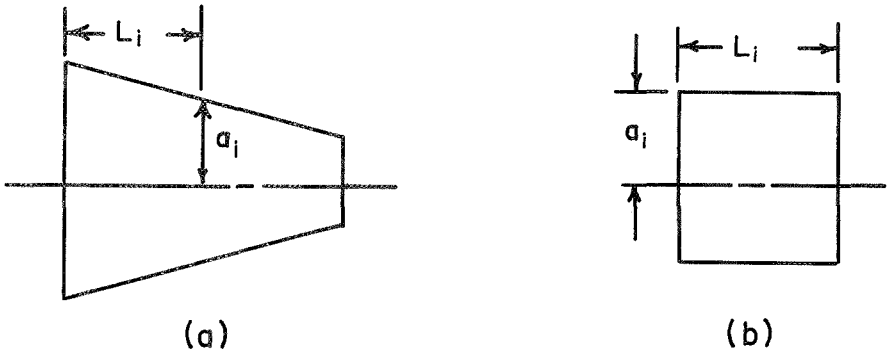

FIGURE 10. TRUNCATED CONICAL SHELL WITH INTERMEDIATE RADIUS a_i AND CORRESPONDING APPROXIMATING CYLINDER

of finite cylindrical segments. It has also been shown that there is a peak in the acoustic radiation efficiency of a cylindrical segment at or near the ring frequency of that segment (Manning and Maidanik, 1962). It is thus concluded that a conical shell can be approximated by a series of cylindrical segments. If the radiation efficiency is determined for these segments at each of their ring frequencies, then the net result will be a series of upper values of radiation efficiency for the conical shell. The net result is what may be called the upper bound solution.

The appropriate lengths of the cylindrical segments are of prime importance. Chandiramani[2] describes the vibrational behavior of the truncated conical shell in a way which facilitates the correct choice of length of the approximating cylinder. He says, in effect, that radiating modes exist in the portion of the conical shell with radius greater than the radius of the segment which has a ring frequency near the frequency of excitation. Thus the length of the corresponding segment at a particular frequency will be the length of the conical shell which possesses modes of vibration. This is the portion of the conical shell which has radius greater than or equal to the radius of the segment whose ring frequency is the excitation frequency.

As an example of the vibrational behavior of the conical shell consider the behavior of the structure shown in Figure 11. The lower ring frequency f_L corresponds to a_1 and the upper ring frequency f_u corresponds to a_2. If the conical shell in Figure 11 is immersed in

---

[2] Ibid.

an acoustic field with excitation frequency, f_i where $f_L \leq f_i \leq f_u$, there is a segment of the conical shell of radius a_i, where $a_2 \leq a_i \leq a_1$ with ring frequency equal to f_i. Then, as previously described, the length of the conical shell with radiating modes is the portion with radius greater than a_i, that is L_i. Using this technique, a cylindrical element is extracted and the acoustic radiation efficiency is calculated for that segment.

Computational Technique for Radiation Efficiency of Truncated Conical Shell

In a way similar to that done for the cylinder, an illustrative example is presented in which the radiation efficiency for a truncated conical shell is computed. This is done under the assumption that the reader understands the cylindrical segment representation previously discussed. The truncated conical shell which will be analyzed is shown in Figure 12a. The structural and acoustic parameters for the shell are presented in Table 2. According to previous discussion, the conical shell will be divided into several cylindrical segments. In the first approximation, the conical shell will be divided up as shown in Figure 12 b, c, d, e, f, g. The ring frequencies corresponding to these segments are shown in Table 3.

The frequencies listed in Table 3 are the frequencies for which values of radiation efficiency will be calculated. Thus, six different values of the radiation efficiency of the truncated conical shell will be computed. These values of radiation efficiency will be the upper bound solutions of the radiation efficiency of the truncated conical shell.

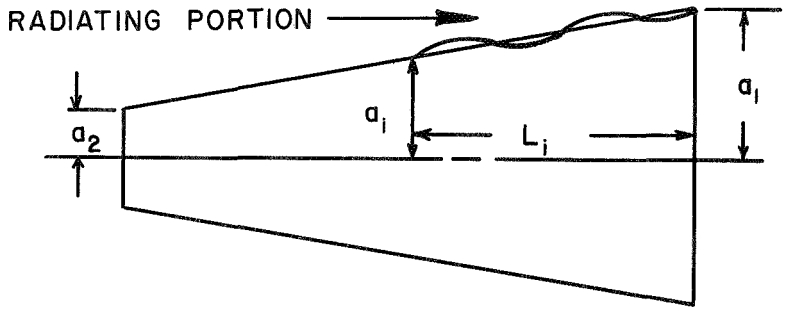

FIGURE 11. TRUNCATED CONICAL SHELL IMMERSED IN A SOUND FIELD WITH EXCITATION FREQUENCY f_i

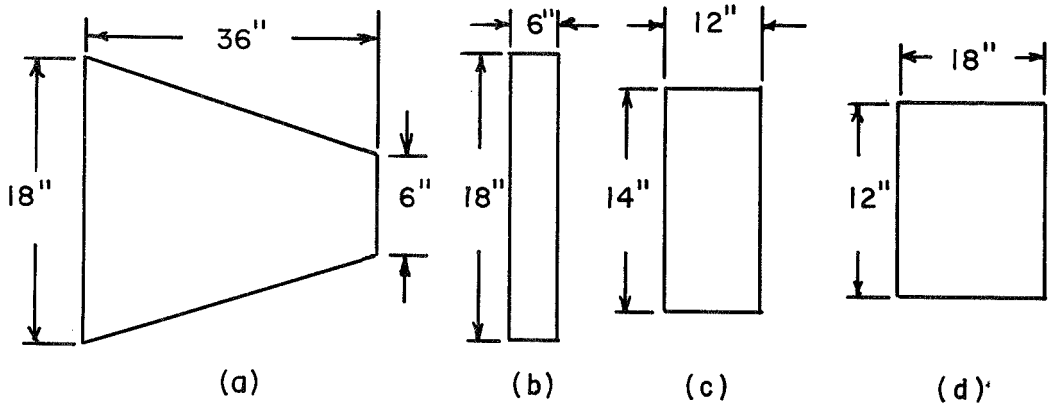

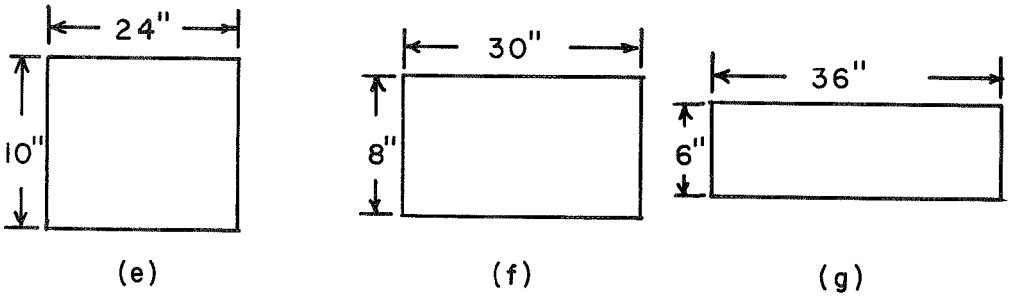

FIGURE 12. EXPERIMENTAL CONICAL SHELL AND APPROXIMATING SEGMENTS

Table 2. Structural and acoustical parameters for experimental conical shell

Shape	Truncated Conical Shell
Material	Stainless Steel 304
Length	36 inches
Smallest Radius	3 inches
Largest Radius	9 inches
Thickness	0.0625 inch
Young's Modulus	27.6×10^6 lb_f/in^2
Density	0.28 lbm/in^3
Lower Ring Frequency	3,450 Hz
Upper Ring Frequency	10,360 Hz
Critical Frequency	7,971 Hz
Velocity of Wave Propagation (C_L)	1.952×10^5 in/sec
Poisson's Ratio	0.3
Medium	Air
Air Density	0.077 lbm/ft^3
Ambient Speed of Sound (c_o)	13,550 in/sec

Table 3. Cylindrical segment ring frequencies

Segment Number	Ring Frequency (Hz)
1	3,885
2	4,440
3	5,179
4	6,215
5	7,729
6	10,360

Consider first the six-inch long segment. The value of σ will be calculated around its ring frequency of 3,885 Hz. The analytical-graphical method for determining the radiation efficiency of a cylinder previously described will be used on this segment. The graph which applies to this particular segment is Figure 13. The actual numbers involved in the calculation of radiation efficiency of the conical shell can be seen in Table 4. The value of n_f is 11 and the value of n_{tot} is 19. Here n_f is the number of acoustically fast modes in the frequency band and n_{tot} is the total number of modes in that same frequency band. Referring to Figure 13 it is noticed that the nearest third-octave center frequency to the ring frequency is chosen as the frequency around which the computation is made. The reason for this is because in the experimental program the conical shell will be excited with one-third octave frequency bands. In this case, the ring frequency is 3885 Hz so the nearest one-third octave center frequency is 4000 Hz. The frequency band ranges from 3540 Hz to 4460 Hz or from $\nu = 0.91$ to $\nu = 1.15$. It is in this band that n_f and n_{tot} are found. If n_f is 11 and n_{tot} is 19 then

$$\sigma|_{3885\ Hz} = n_f / n_{tot} = 0.58 \quad . \tag{44}$$

This is the value of radiation efficiency of that cylindrical segment at 3885 Hz and is by definition the upper-bound value of radiation efficiency of the truncated conical shell at 3885 Hz.

In the same manner and using Figures 14, 15, 16, 17, 18, 19, n_f and n_{tot} were found for segments 2, 3, 4, 5, and 6, shown in Figure 12, and their radiation efficiencies were found. This comprised the first

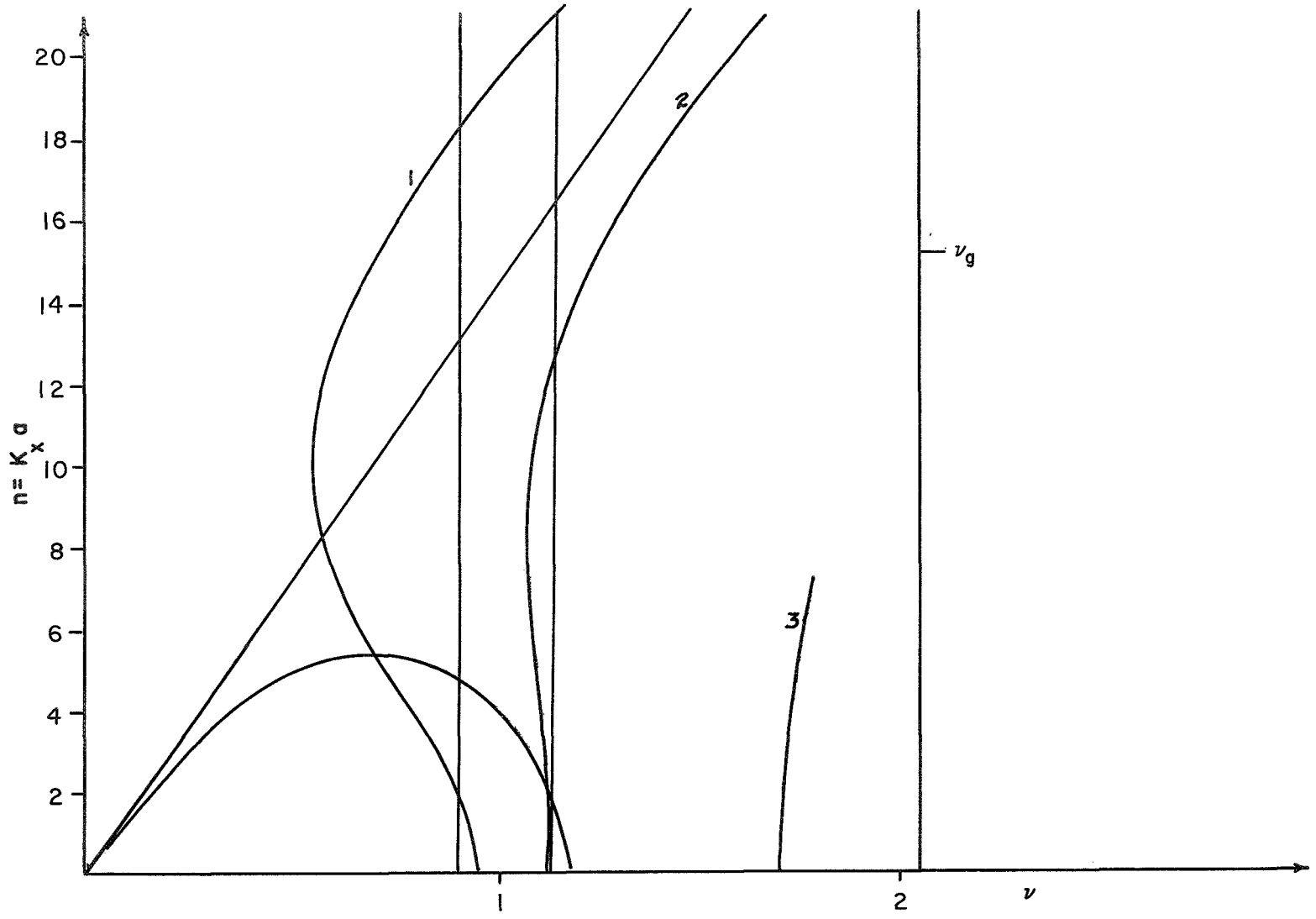

FIGURE 13. RADIATION EFFICIENCY CALCULATION GRAPH FOR A 6-INCH CYLINDRICAL SEGMENT

Table 4. Values of n_f and n_{tot} for cylindrical segments as a function of length

Segment Length (inches)	N_f	N_{tot}
2	0	0
3	14	14
4	0	8
6	11	19
8	2	13
9	6	17
10	9	23
12	2	21
14	11	28
15	9	28
16	13	36
18	11	36
20	11	42
21	16	48
24	13	53
26	14	50
27	13	54
28	39	68
30	*[a]	*[a]
32	*[a]	*[a]
33	*[a]	*[a]
36	*[a]	*[a]

[a] * For these lengths $n_f \approx n_{tot}$.

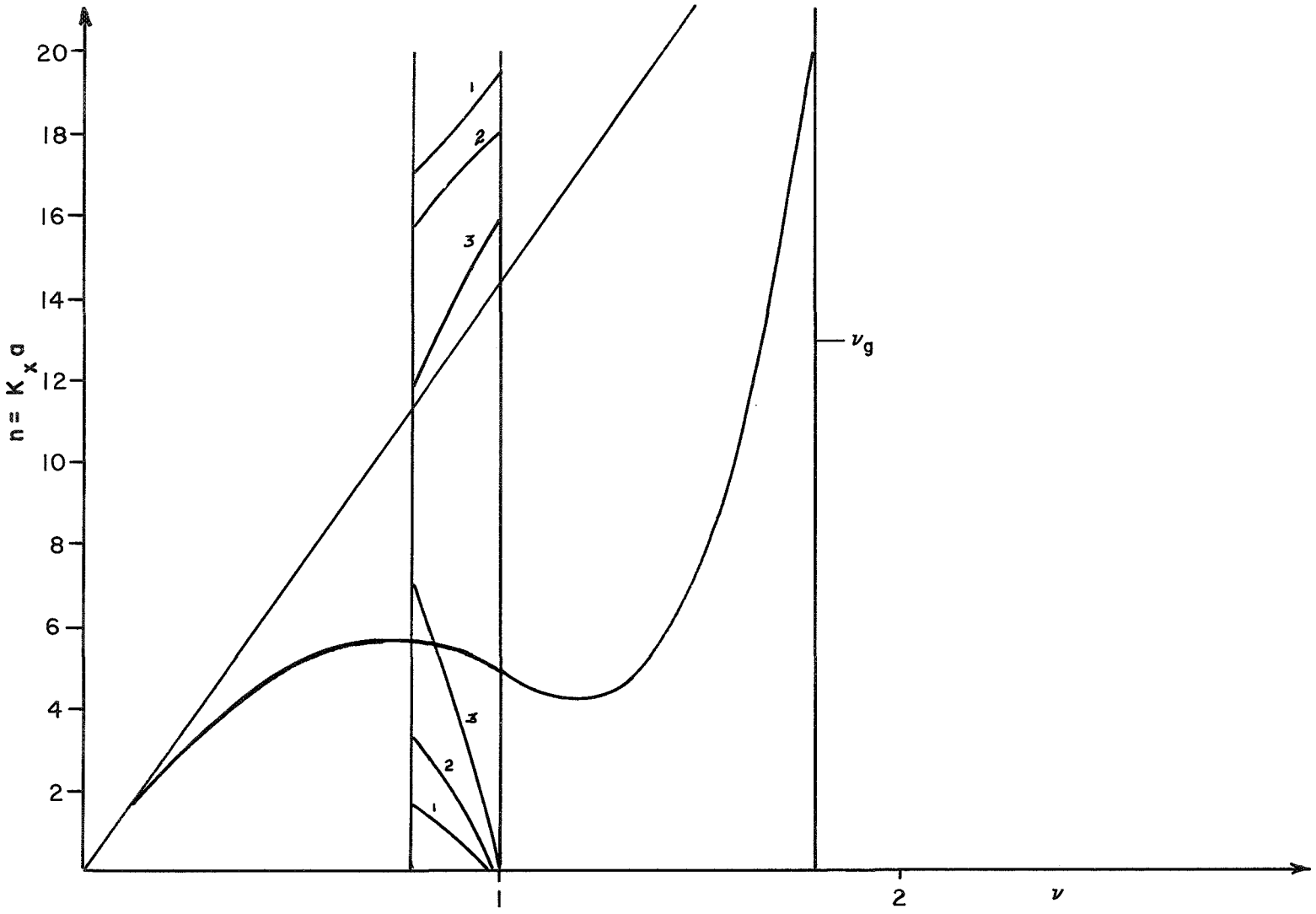

FIGURE 14. RADIATION EFFICIENCY CALCULATION GRAPH FOR A 12-INCH CYLINDRICAL SEGMENT

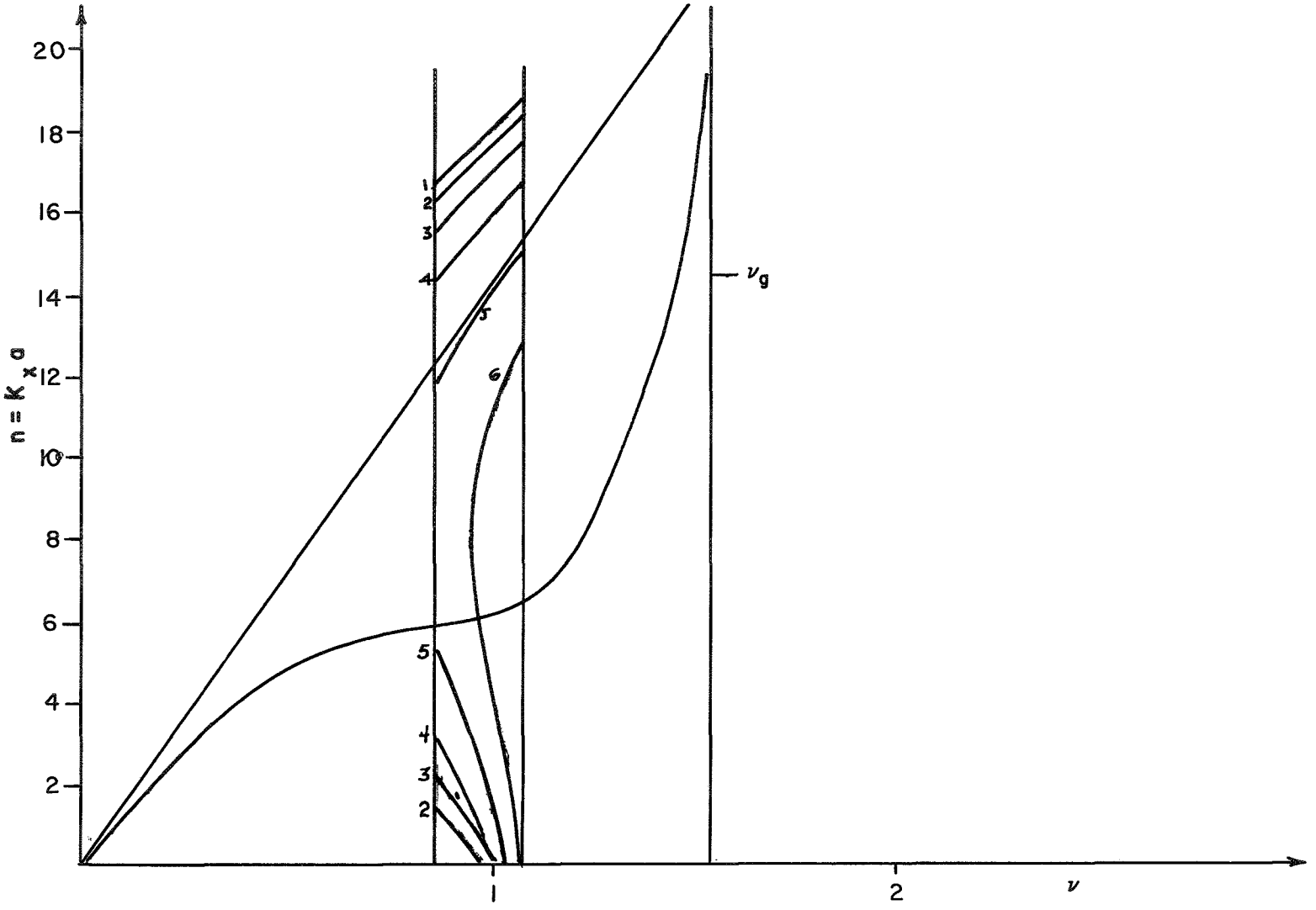

FIGURE 15. RADIATION EFFICIENCY CALCULATION GRAPH FOR AN 18-INCH CYLINDRICAL SEGMENT

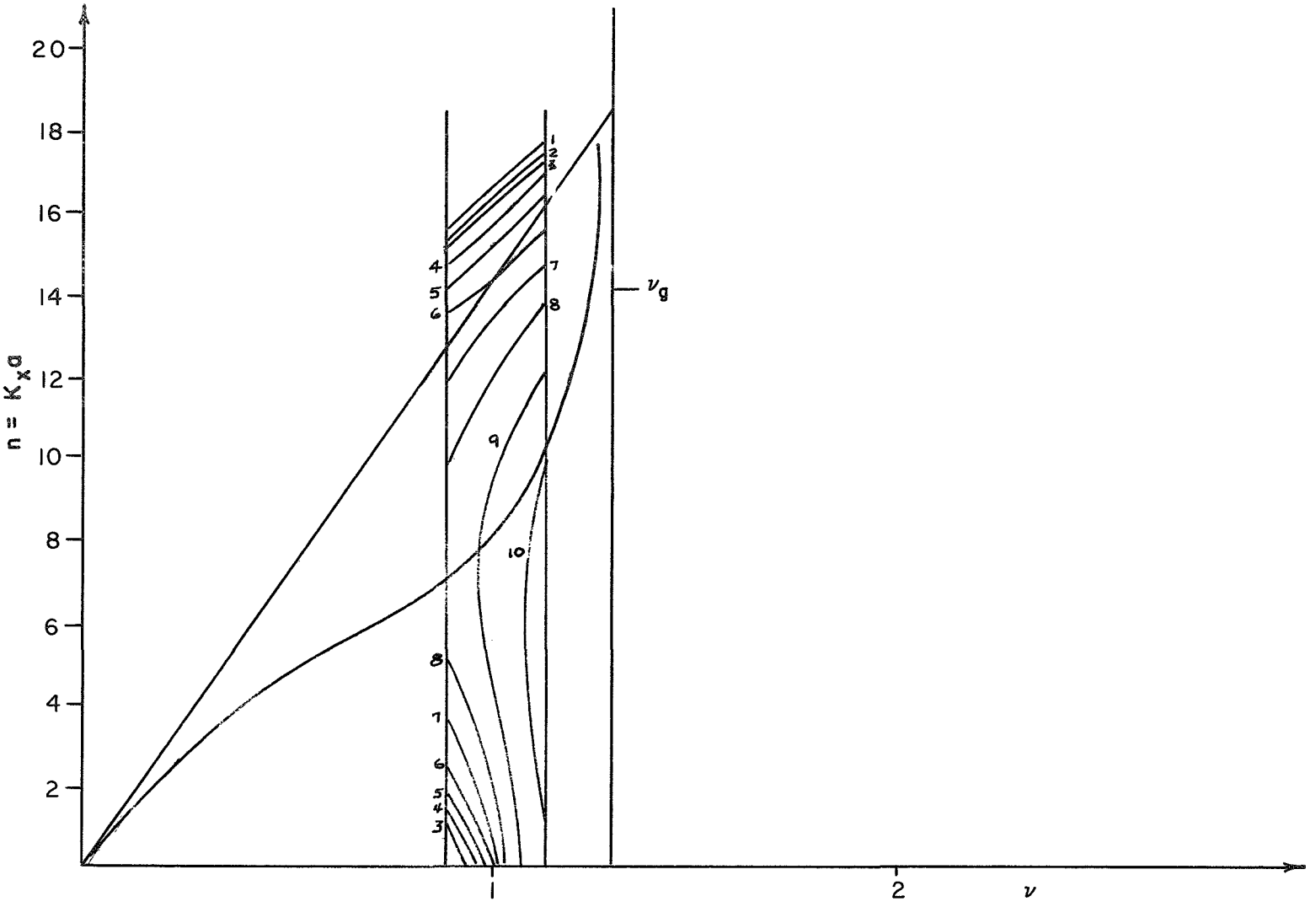

FIGURE 16. RADIATION EFFICIENCY CALCULATION GRAPH FOR A 24-INCH CYLINDRICAL SEGMENT

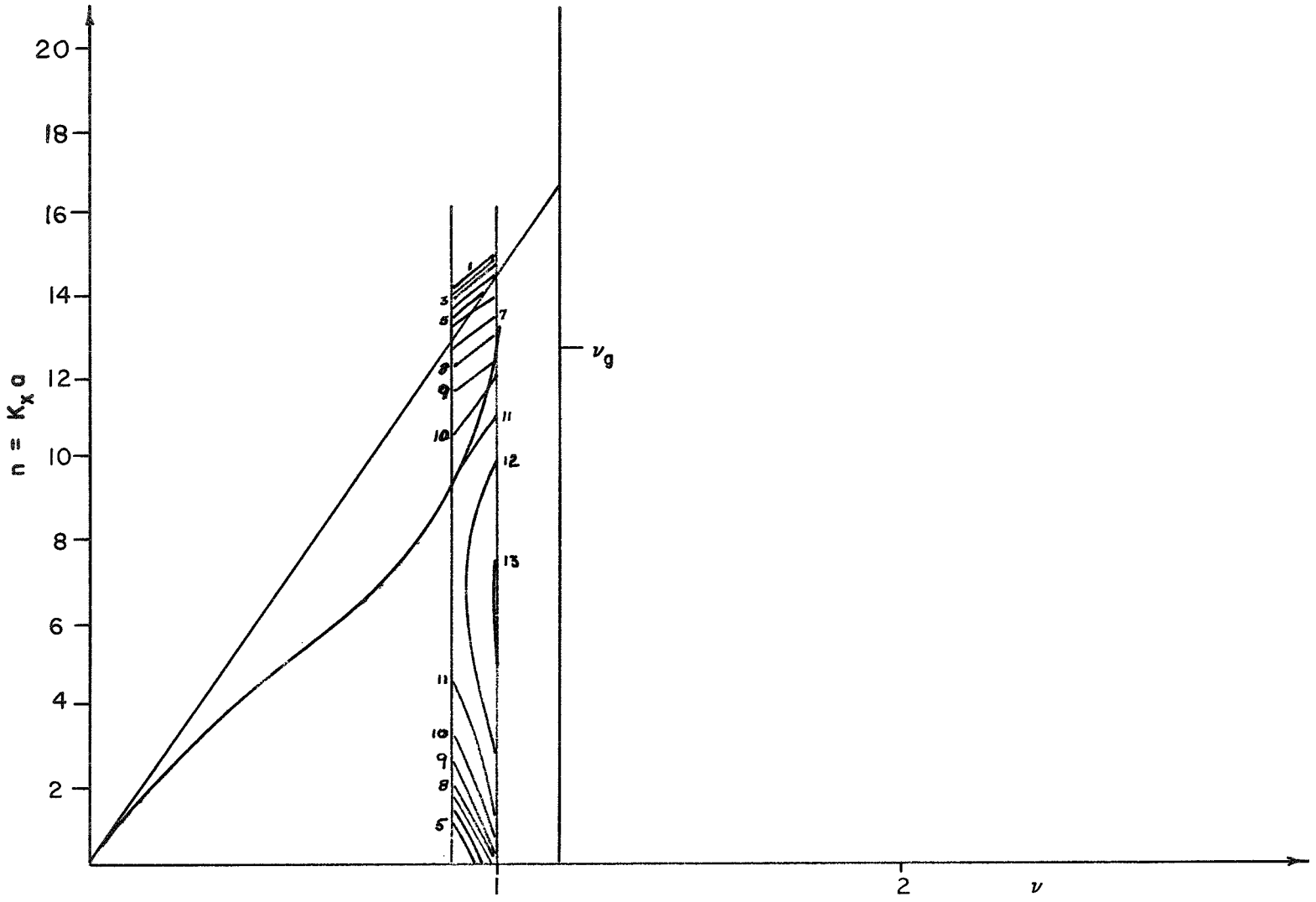

FIGURE 17. RADIATION EFFICIENCY CALCULATION GRAPH FOR A 30-INCH CYLINDRICAL SEGMENT

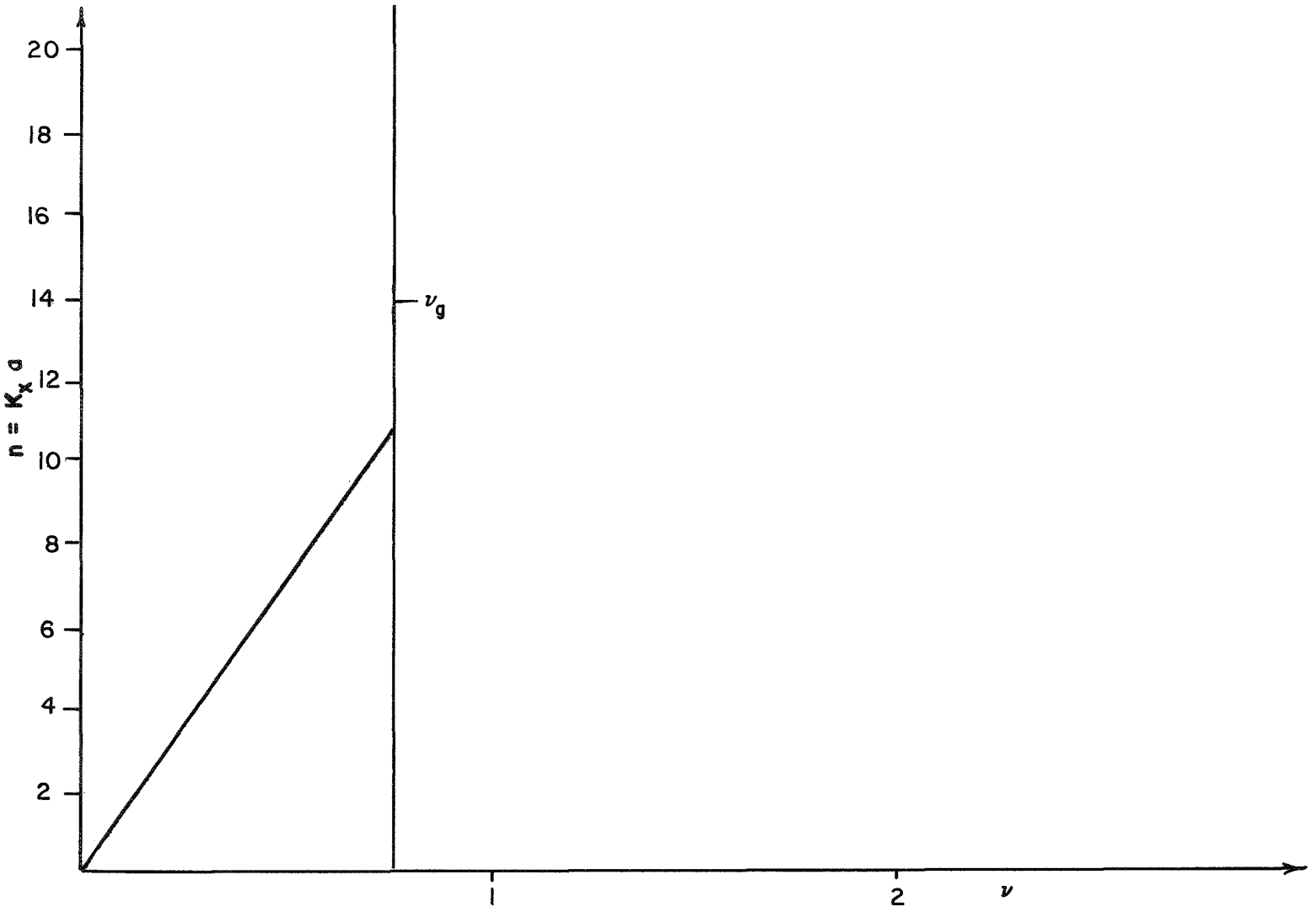

FIGURE 18. RADIATION EFFICIENCY CALCULATION GRAPH FOR A 36-INCH CYLINDRICAL SEGMENT

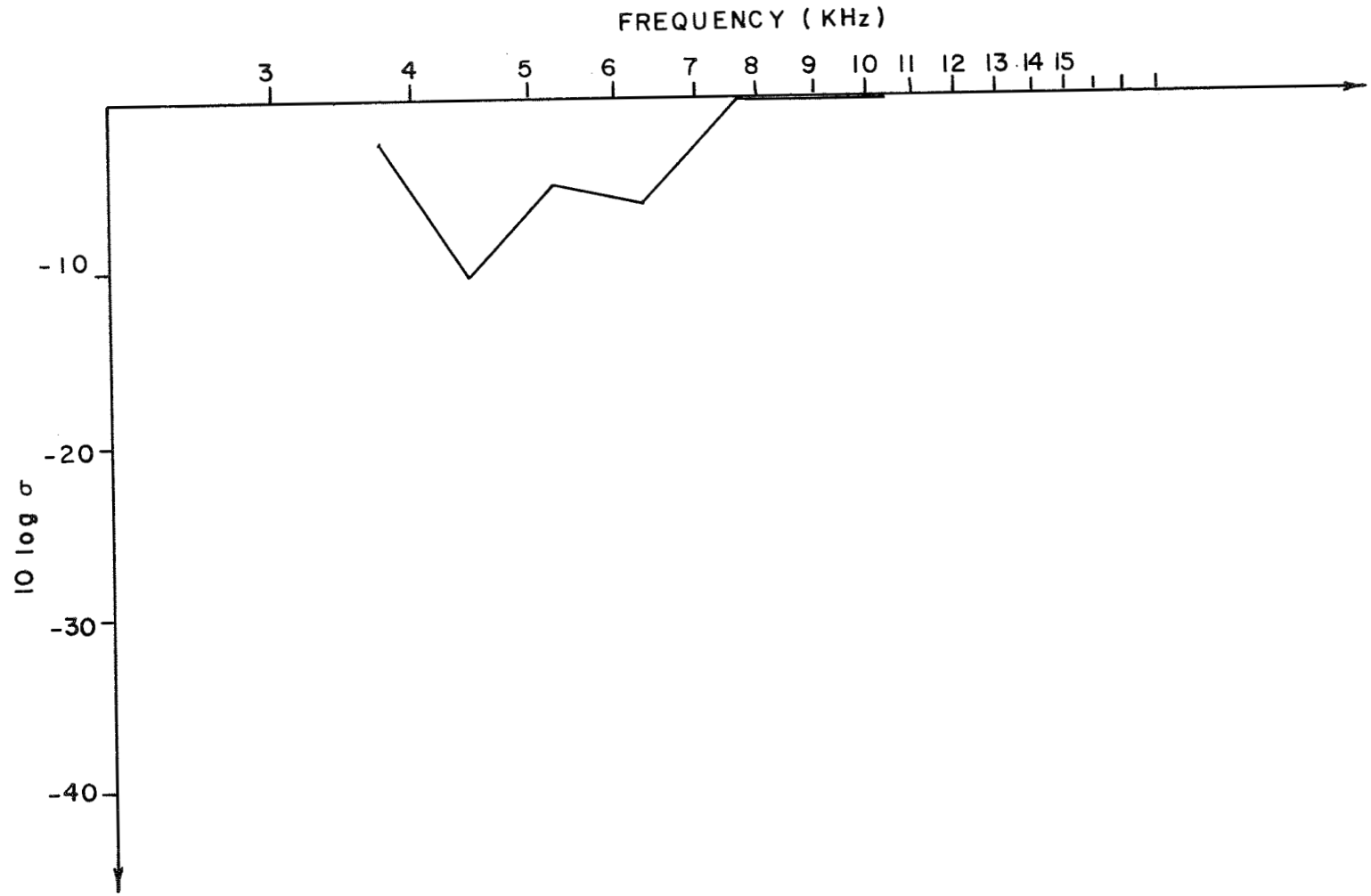

FIGURE 19. THEORETICAL RADIATION EFFICIENCY FOR TRUNCATED CONICAL SHELL DIVIDED INTO 6 SEGMENTS

set of results for the upper bound solution of acoustic radiation efficiency of the truncated conical shell. These results are plotted in Figure 19.

Next, the conical shell is approximated by nine segments, equally incremented in length from four inches to thirty-six inches by four-inch increments. A more precise solution is gained by approximating the conical shell in smaller increments. The results of this approximation are plotted in Figure 20.

A still smaller length increment of three inches is chosen for the next approximation. The cone is approximated first by a three-inch length segment and incremented by three inches each. The cone is thus approximated by twelve segments. The results of this approximation are plotted in Figure 21.

Finally, as the most precise approximation, the cone was approximated by eighteen cylindrical segments. The first cylindrical segment was two inches in length and the length was increased by two inches in each approximation. The results of this approximation appear on Figure 22. Figures 19, 20, 21, and 22 comprise the upper bound solutions for the acoustic radiation efficiencies of the truncated conical shell.

The radiation efficiency of most any truncated conical shell can be computed by this method. The only modifications which have to be made in the procedure are for the differing structural parameters of the truncated conical shell to be analyzed.

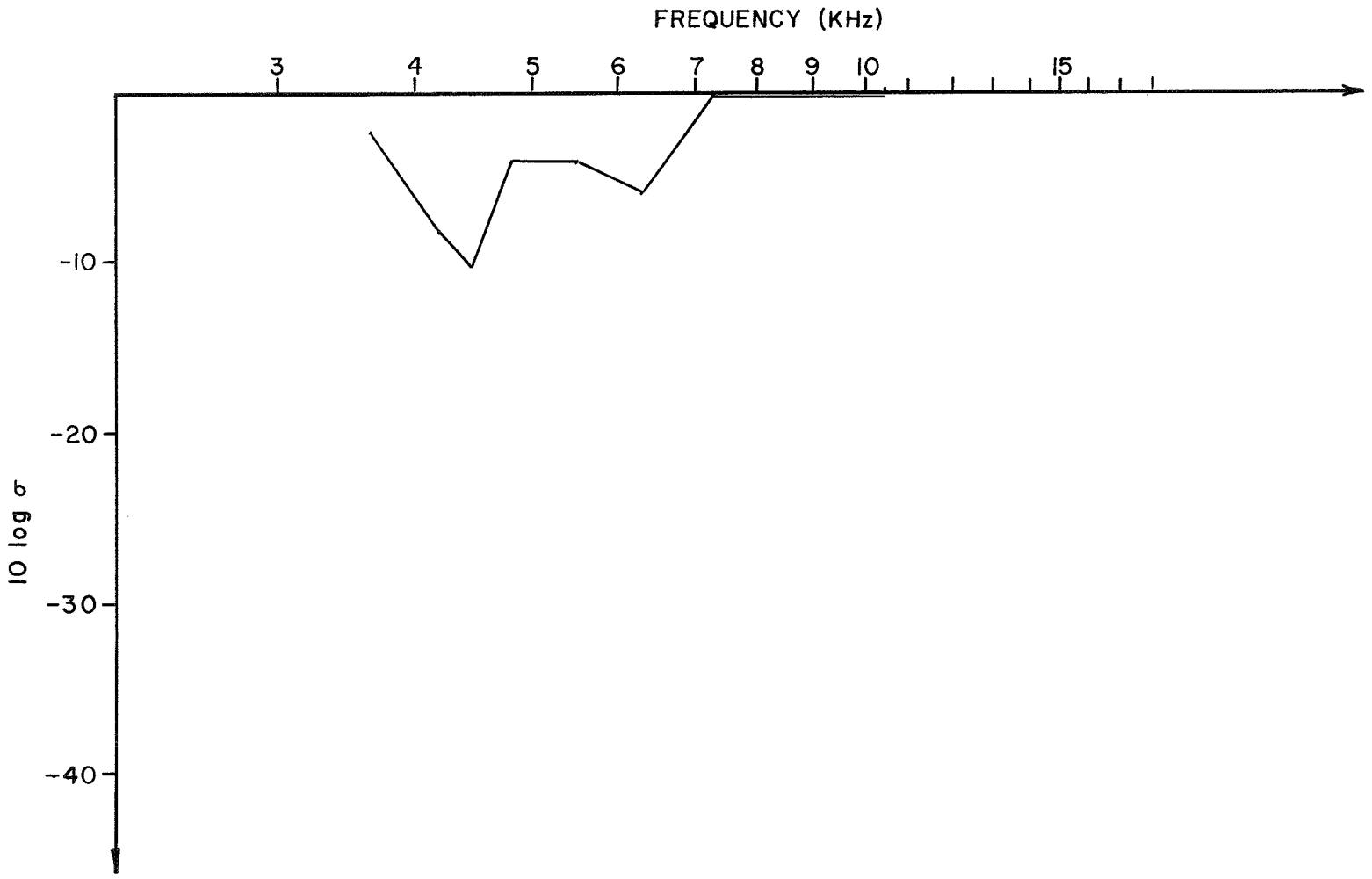

FIGURE 20. THEORETICAL RADIATION EFFICIENCY FOR TRUNCATED CONICAL SHELL DIVIDED INTO 9 SEGMENTS

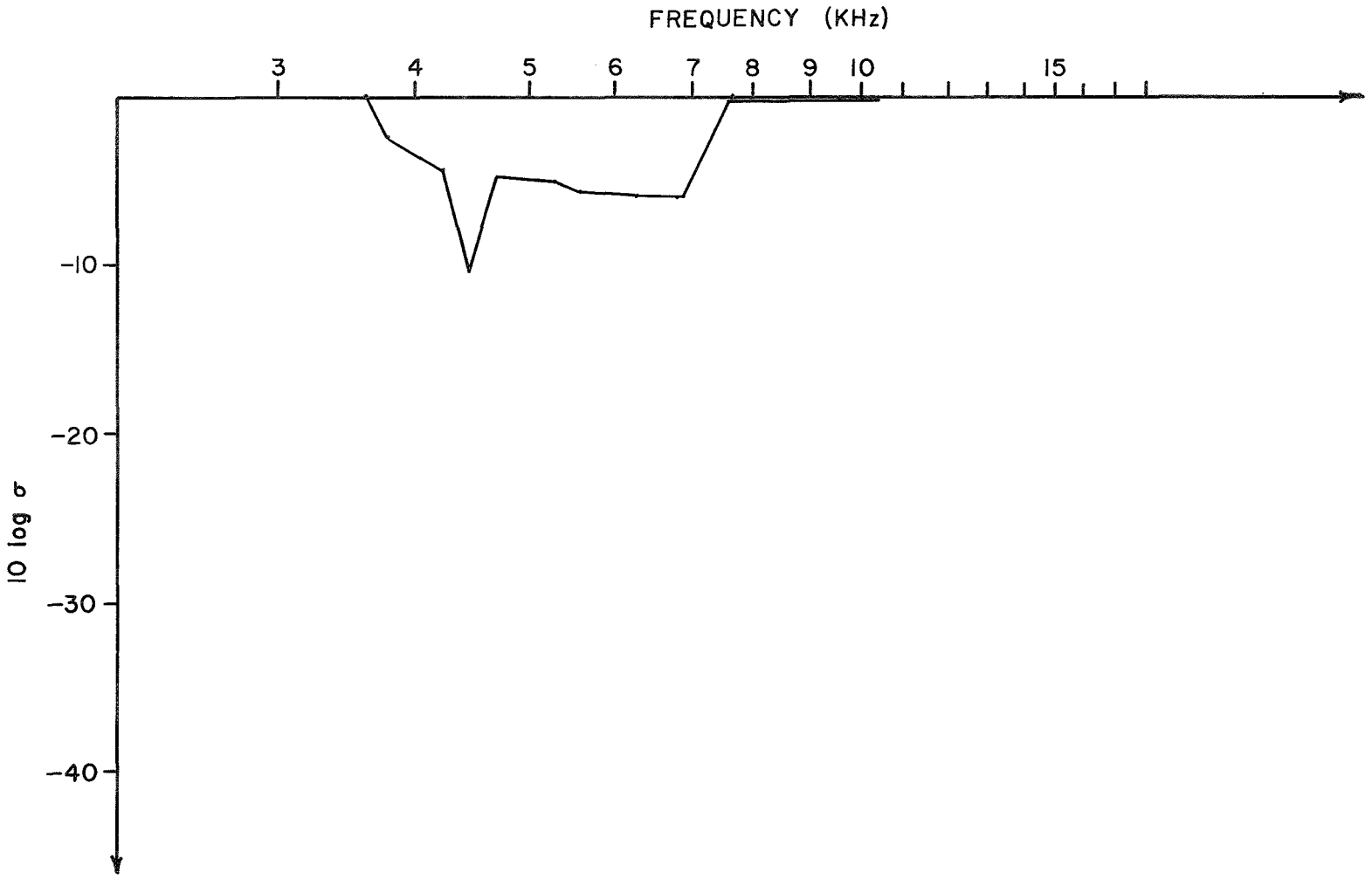

FIGURE 21. THEORETICAL RADIATION EFFICIENCY FOR TRUNCATED CONICAL SHELL DIVIDED INTO 12 SEGMENTS

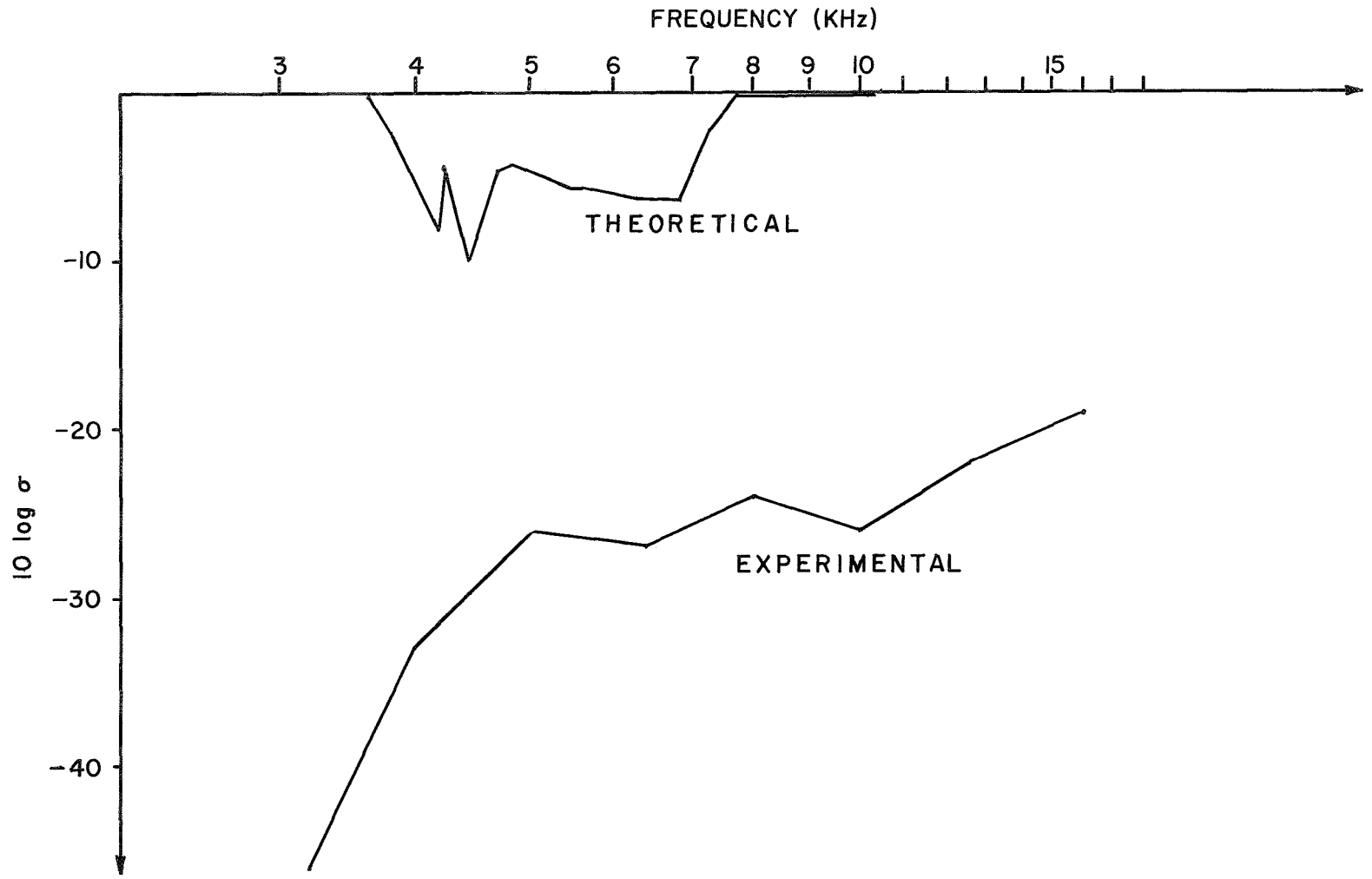

FIGURE 22. THEORETICAL AND EXPERIMENTAL RADIATION EFFICIENCY OF TRUNCATED CONICAL SHELL DIVIDED INTO 18 SEGMENTS

EXPERIMENTAL INVESTIGATION

Experimental Analysis of Parameters

Maidanik (1962) extensively investigated the response of ribbed panels to reverberant acoustical fields. This work led to the development and use of certain experimental equations which are valuable not only in evaluating the radiative properties of panels, but which work well on shell structures. These equations will be applied to the experimental analysis of truncated conical shells. The purpose is to determine experimental values of radiation efficiency with which to compare to the theoretical results. The concern is on the acoustic radiation to and from a structure immersed in a diffuse sound field which is assumed to be reverberant (see Figure 26).

Lyon and Maidanik (1962) note that, under the assumption of equipartition of energy, it can be shown that

$$\frac{S_a(\omega)}{S_p(\omega)} = \left\{ \frac{2\pi^2 n_p(\omega)}{M_p} \right\} \frac{c_o}{\rho_o} \left\{ \frac{R_{rad}}{R_{rad} + R_{mech}} \right\} . \tag{43}$$

This equation was originally developed for flat panels but it can also apply to shell structures as well.

The coupling factor of a structure expresses the ratio of energy radiated acoustically by a structure to the amount of vibrational energy received by the structure. The coupling factor is defined to be μ', where

$$\mu' = \frac{\text{Power Radiated}}{\text{Total Amount of Power Dissipated}} \tag{44}$$

or,

$$\mu' = \frac{R_{RAD}}{R_{RAD} + R_{MECH}} \tag{45}$$

Note that equation (45) is the last term in equation (43). Conceptually μ' can be illustrated in a simple diagram (see Figure 23). Figure 23 shows an arbitrary structure receiving vibrational energy of the amount E, radiating an amount $\mu'E$, and storing, or dissipating, an amount $(1-\mu')E$. If equation (45) is substituted into equation (43) the relation becomes

$$\mu(\omega) = \left[\frac{S_a(\omega)}{S_p(\omega)} \right] \left[2\pi^2 \left(\frac{n_s(\omega)}{M_s} \right) \frac{c_o}{\rho_o} \right]^{-1} . \tag{48}$$

The radiation resistance R_{rad} must now be determined. The experimental equation developed by Lyon and Maidanik (1962) is:

$$R_{rad} = \left[\frac{S_p(\omega)}{S_a(\omega)} \right] \left[2\pi^2 \beta_R n_R(\omega) \right] \frac{c_o}{\rho_o} \tag{49}$$

where

$$\beta_R = \frac{13.8}{T_R} . \tag{50}$$

After finding R_{rad} from equation (49), the radiation efficiency can be calculated and is seen to be

$$\sigma = \frac{R_{rad}}{\rho_o c_o A} \tag{51}$$

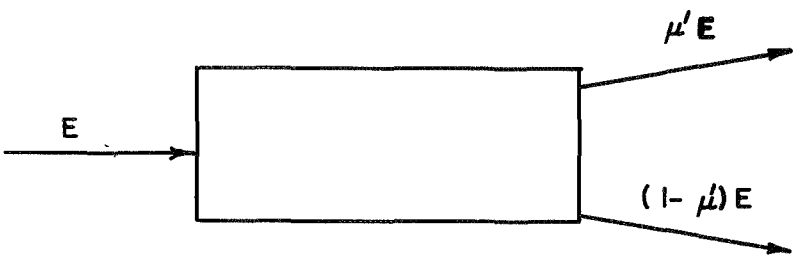

FIGURE 23. ARBITRARY STRUCTURE RECEIVING ACOUSTIC ENERGY

To find the total resistance $R_{rad} + R_{mech}$, the structure must be excited by a diffuse sound field and equation (48) must be used. To find R_{rad}, the structure is excited by a mechanically coupled shaker and the structure excites a field in a room. The result is that the structure is immersed in a reverberant sound field. Equation (49) is then used to find R_{rad} and equation (51) is used to find σ. Thus, when the parameters of equation (49) are found, then an experimental solution for the radiation resistance and efficiency is available. This experimental method will be used to investigate the theoretical solution.

Measurement of Radiation Resistance

Measurement of Acceleration Power Spectral Density

The subject of this section is a discussion of the aspects of measurement of the acceleration power spectral density of the vibrating truncated conical shell. The Bruel and Kjaer Company (1966) presents a manual on the determination of power spectral density with respect to both acceleration and sound pressure. In this manual is outlined theory on the subject of power spectral density as well as practical applications to the determination of power spectral density.

In order to experimentally determine the acceleration power spectral density for the truncated conical shell, the shell was mounted in a simulated free-free boundary condition. An accelerometer (B and K type 4336) was attached to the conical shell in a random position. An electromechanical shaker (MB No. EA 1250) was mechanically clamped to the conical shell near the large end of the shell providing the

vibrational excitation (see Figure 24). The shaker was driven by its counterpart power amplifier (MB No. 2120). This power amplifier was driven by the signal from a random-noise generator (B and K type 1402) which was filtered by a third-octave filter (B and K type 1612). The accelerometer output fed into a cathode follower (B and K type 2615) through a microphone cable to a microphone amplifier (B and K type 2603) which indicated the voltage output of the accelerometer (see Figure 25). The entire cone structure and shaker was positioned in a test facility whose sound field was considered to be reverberant (see Figure 26). The electronic instrumentation (see Figure 25) was placed in a room adjoining the test facility. The reason that the electronic instrumentation was not located in the test chamber was because its presence would contribute to sound absorption and thus lower the reverberance of the sound field. Figure 25 shows all the instrumentation needed for the complete experimental determination of radiation efficiency. Summarizing, the procedure followed to determine the acceleration power spectral density is:

(1) Install all equipment;

(2) Excite the system with filtered random noise through several frequencies;

(3) Record the output of the accelerometer.

Then $S_a(\omega)$ can be found as a function of frequency.

Measurement of Sound Pressure Power Spectral Density

The experimental determination of the sound pressure power spectral density was very similar to the determination of acceleration power spectral density. The main difference between the two was that

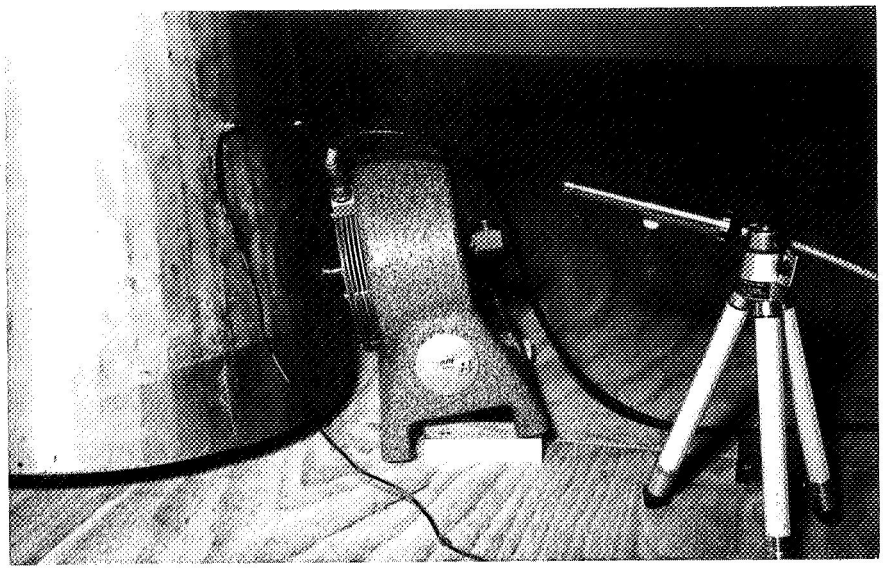

FIGURE 24. EXPERIMENTAL APPARATUS TO EXCITE CONICAL SHELL AND RECORD ACCELERATION AND SOUND PRESSURE

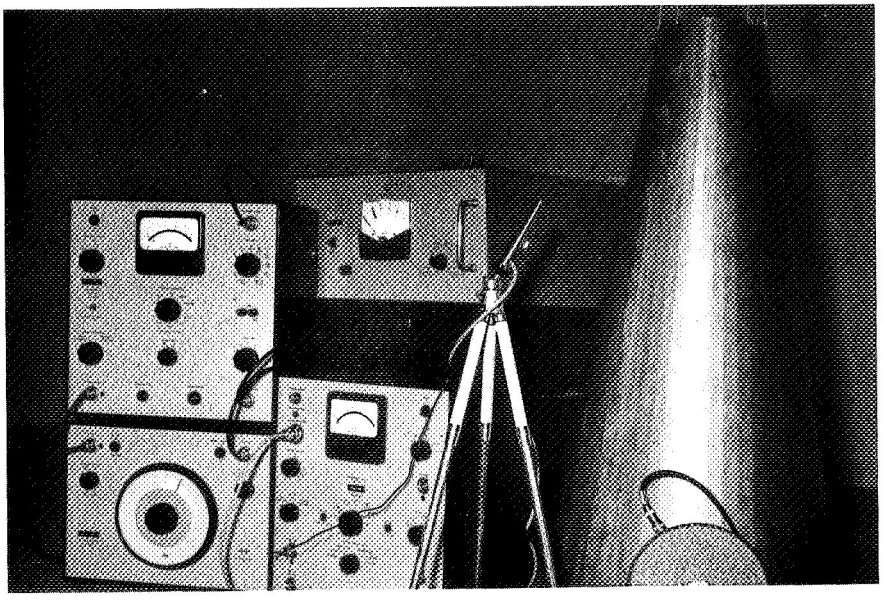

FIGURE 25. INSTRUMENTATION AND APPARATUS USED IN EXPERIMENTAL PROGRAM

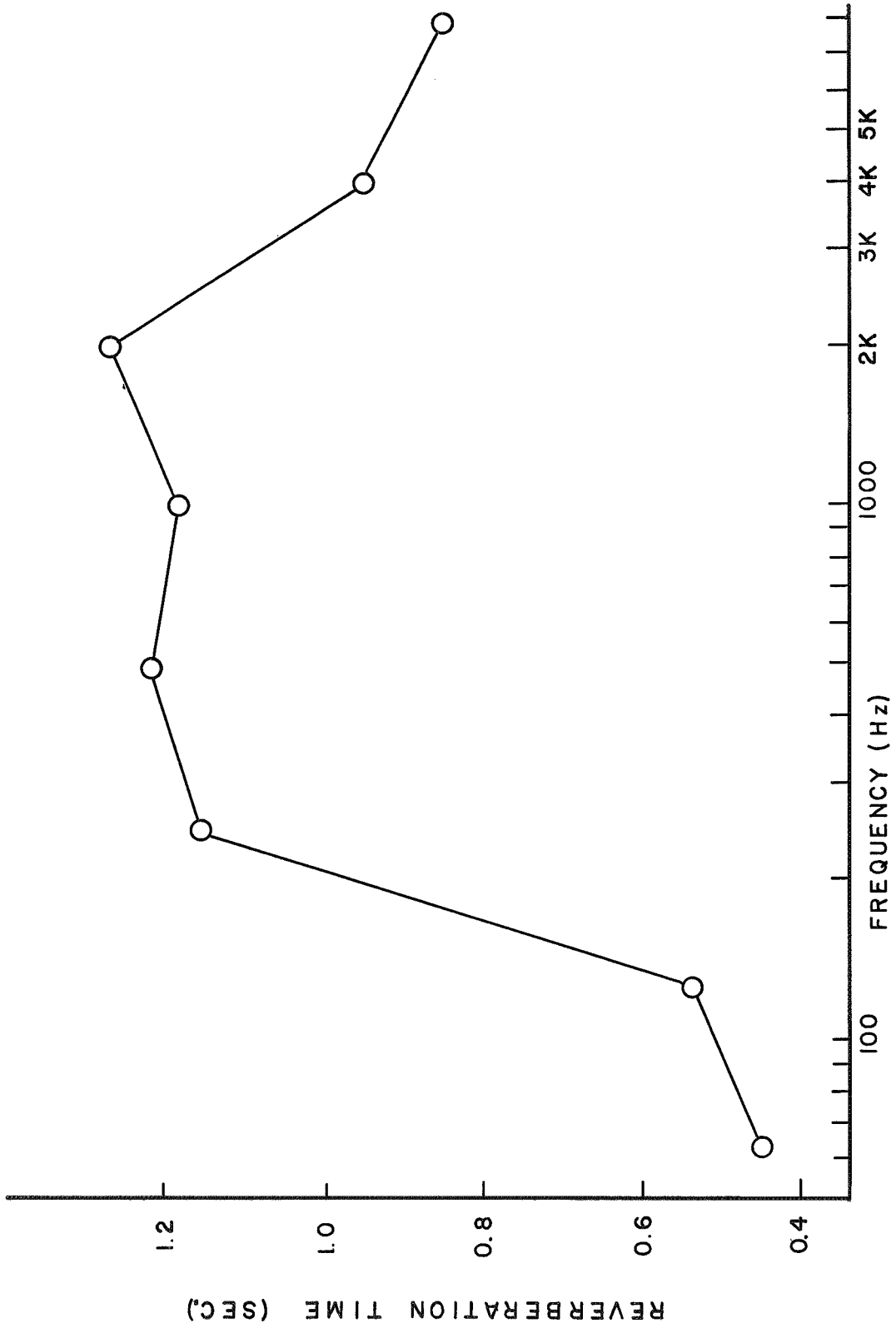

FIGURE 26. REVERBERATION TIME OF TEST FACILITY

instead of using an accelerometer as a transducer, a microphone (B and K type 4134) was the transducer. The procedure otherwise was identical and the power spectral density spectrogram as a function of frequency was similar.

Measurement of Reverberation Time of Acoustic Field

The reverberation time of the test facility was determined by exciting the facility with random noise filtered in octaves. The excitation was provided by exciting two audio amplifiers with the octave-band signal. These amplifiers drove two speaker systems in the test facility. At a particular instant, the excitation was terminated and the time was recorded for the acoustic energy in the room to drop by 60 dB. This time, in seconds, is defined as the reverberation time at a particular octave frequency. The results of the reverberation measurements appear in Figure 26. This figure shows reverberation time as a function of frequency.

Measurement of Modal Density of Acoustic Field

The cumulative number of resonances below a certain frequency in a rectangular enclosure has been given by Morse and Bolt (1944). The modal density of a rectangular enclosure is presented in equation (20). This equation results from taking the partial derivative with respect to frequency of the cumulative number of modes below a certain frequency in a rectangular enclosure. The modal density of the rectangular test facility is the modal density of the reverberant field which exists in the facility. Thus the modal density of the reverberant field is not affected by the modal density of the structure immersed in the

field. This statement can be partially justified by the fact that, at higher frequencies, such as the ones in this experimental investigation, the modes of the acoustic field and those of the structure are essentially uncoupled.

Experimental Results

The results of the experimental program are seen on Figure 22. This figure shows eight data points of the acoustic radiation efficiency. The experimental results verify the fact that the acoustic radiation efficiency increases with increasing ka. These results are found at 1/3 octave center frequencies which can be seen on the abcissa of Figure 22. These results are plotted in the customary way of representing radiation efficiency, that is, in terms of 10 log σ.

COMPARISON OF EXPERIMENTAL AND THEORETICAL RESULTS

The results of both the most precise theoretical investigation and the experimental investigation can be seen in Figure 42. This figure shows that there is a significant difference between the theoretical results and the experimental results. The difference between the two is greater at the lower frequencies than at the higher frequencies. The difference is a maximum of 37 at 3650 Hz and a minimum of 19 at 16 KHz. These differences are attributed to the fact that there were distinct inadequacies in the facilities used in the experimental investigation. These inadequacies centered around the fact that the test room was not a reverberation chamber.

SUMMARY AND CONCLUSIONS

The results of both the theoretical and experimental investigations are seen in Figure 22. The theoretical method or analytical-graphical method, based on statistical energy concepts, has been used after approximating the truncated conical shell by a number of discrete cylindrical segments. Using this technique yielded a set of values of radiation efficiency which are defined to be for the truncated conical shell. Because each of the determinations of radiation efficiency of the approximating cylindrical segments were made at the ring frequency of each, an upper bound solution set was obtained. The experimental program was carried out with the intent to verify the upper bound solution of the acoustic radiation efficiency. The experimental program verified the fact that the theoretical solution was an upper bound solution although these were significant differences between the two sets of results.

In conclusion it may be said that the analytical-graphical technique did determine an upper bound solution since none of the experimental results exceeded the theoretical solutions. It must be said however that the parameters which governed the experimental equation were all determined under the assumption that the sound field in which the structure was tested was diffuse. Because of the construction of the test facility, it is observed that the test facility does not meet the qualifications of a reverberation chamber. Thus the sound field will not be completely diffuse. In this case, acoustic energy will be lost through the room's boundaries and will not be reflected back to

the excited structure. Any acoustic energy which is lost will lower the sound pressure power spectral density which appears in the numerator of the relation for acoustic radiation efficiency. Thus if that term is lowered, the net result will be a lowering of the radiation efficiency if all the other parameters of the equation are held constant. It is felt that this is the main reason that the experimental results are so much lower than the theoretical results. The author recommends that all tests of this sort should be made in a reverberation chamber of high quality.

Knowledge of the acoustic radiation efficiency and acoustic radiation resistance of a body is very useful. Knowing this parameter will facilitate an evaluation of the energy dissipated in a structure which receives acoustic or vibrational energy. Also, the amount of energy radiated from a structure which receives vibrational energy is directly dependent upon radiation efficiency and radiation resistance. A method which determines the acoustical radiation efficiency of a truncated conical shell is of prime importance because of the widespread use of the truncated conical shell structure in engineering and science.

LIST OF REFERENCES

Bruel and Kjaer Instruments, Inc. 1966. Application of B and K Equipment to Frequency Analysis and Power Spectral Density Measurements. K. Larsen and Son, Lyngby, Denmark.

Heckl, M. 1962. Vibration of point-driven cylindrical shells. J. Acoust. Soc. Am. 34(10):1553-1557.

Kinsler, Lawrence E. and Frey, Austin R. 1962. Fundamentals of Acoustics. John Wiley and Sons, Inc., New York, New York.

Lyon, Richard H. and Maidanik, Gideon. 1962. Power flow between linearly coupled oscillators. J. Acoust. Soc. Am. 34(5):623-639.

Maidanik, Gideon. 1962. Response of ribbed panels to reverberant acoustic fields. J. Acoust. Soc. Am. 34(6):809-826.

Manning, Jerome E. and Maidanik, Gideon. 1964. Radiation properties of cylindrical shells. J. Acoust. Soc. Am. 36(9):1691-1698.

Miller, David K. 1969. Density of eigenvalues in thin circular conical shells. Unpublished Ph.D. thesis, Department of Mechanical and Aerospace Engineering, North Carolina State University at Raleigh, North Carolina.

Morse, P. M. and Bolt, R. H. 1944. Sound waves in rooms. Rev. Mod. Phys. 16(2):69-150.

APPENDIX. LIST OF SYMBOLS

A = area of structure

a = radius of structure

C_B = bending-wave speed

C_L = longitudinal-wave speed

c = speed of sound

c_o = ambient speed of sound

Cir = circumference

E = Young's Modulus

E_R = acoustic energy

f = frequency (Hz)

f_g = critical frequency

f_i = intermediate ring frequency

f_L = lower ring frequency

f_r = ring frequency

$\bar{f}_r$ = reaction force on piston

f_u = upper ring frequency

h = thickness of structure

I = radiation intensity

K = Boltzmann's constant

k = wave number

K_x = circumferential wave number

K_y = axial wave number

L_i = length of arbitrary segment

L = length of cylinder or conical shell

M_p = panel mass

m = axial mode number

n = circumferential mode number

n_f = number of acoustically fast modes

$n_p(\omega)$ = panel modal density

$n_R(\omega)$ = modal density of room

$n_S(\omega)$ = structure modal density

n_{tot} = total number of modes

P = acoustic pressure

$\bar{P}$ = pressure on piston

P_{rms} = rms pressure on piston

R_{mech} = mechanical resistance

R_{rad} = radiation resistance

$R_1(x)$ = piston radiation resistance function

r = distance from dS to dS'

S_a = acceleration power spectral density

S_p = sound pressure spectral density

T = temperature

T_R = reverberation time of room

t = time

U_o = velocity amplitude of structure

u = velocity of structure

V = volume of rectangular enclosure

W = average power generated

$X_1(x)$ = piston radiation reactance function

x = 2ka

y = cylindrical segment length

Z_r = radiation impedance

β_r = room time decay constant

θ = angular distance

θ^R = thermal energy

$\theta^R(\omega)$ = average energy per mode in room

$\theta^S(\omega)$ = average energy per mode in structure

λ = wavelength

λ_x = circumferential wavelength

λ_y = axial wavelength

μ = Poisson's ratio

μ' = coupling factor

ν = dimensionless frequency

ν_g = dimensionless critical frequency

ρ_o = ambient air density

σ = radiation efficiency

σ_f = radiation efficiency of acoustically fast mode

ω = angular frequency